

**JAERI-Review
95-002**



**ANNUAL REPORT OF THE
OSAKA LABORATORY FOR RADIATION CHEMISTRY
JAPAN ATOMIC ENERGY RESEARCH INSTITUTE**

(No. 27)

April 1, 1993 - March 31, 1994

March 1995

Osaka Laboratory for Radiation Chemistry

**日本原子力研究所
Japan Atomic Energy Research Institute**

本レポートは、日本原子力研究所が不定期に公刊している研究報告書です。
入手の間合わせは、日本原子力研究所技術情報部情報資料課（〒319-11 茨城県那珂郡東海村）あて、お申し越しください。なお、このほかに財団法人原子力弘済会資料センター（〒319-11 茨城県那珂郡東海村日本原子力研究所内）で複写による実費頒布をおこなっております。

This report is issued irregularly.

Inquiries about availability of the reports should be addressed to Information Division, Department of Technical Information, Japan Atomic Energy Research Institute, Tokaimura, Naka-gun, Ibaraki-ken 319-11, Japan.

© Japan Atomic Energy Research Institute, 1995

編集兼発行 日本原子力研究所
印 刷 いばらき印刷(株)

Annual Report of the
Osaka Laboratory for Radiation Chemistry
Japan Atomic Energy Research Institute
(No. 27)
April 1, 1993 - March 31, 1994

Osaka Laboratory for Radiation Chemistry
Takasaki Radiation Chemistry Research Establishment
Japan Atomic Energy Research Institute
Mii-minami-machi, Neyagawa-shi, Osaka-fu

(Received January 31, 1995)

The annual research activities of Osaka Laboratory for Radiation Chemistry, JAERI during the fiscal year of 1993 (April 1, 1993 - March 31, 1994) are described.

The research activities were conducted under the two research programs; the study on laser-induced organic chemical reactions and the study on basic radiation technology for functional materials. Detailed descriptions of the activities are presented in the following subjects: laser-induced organic synthesis, modification of polymer surface by laser irradiation, radiation-induced polymerization, preparation of fine particles by gamma ray irradiation, and electron beam dosimetry. The operation report of the irradiation facilities is also included.

Keywords: Excimer Laser, Electron Beam, γ -ray, Photochemical Reaction, Polymer Modification, Polymerization, Dosimetry

日本原子力研究所大阪支所年報 (No.27)

1993年4月1日-1994年3月31日

日本原子力研究所高崎研究所

大阪支所

(1995年1月31日受理)

本報告書は、大阪支所において平成5年度に行われた研究活動を述べたものである。主な研究題目は、レーザー光による有機合成、レーザー光による高分子表面改質、電子線照射による重合反応の研究、 γ 線照射による微粒子の生成に関する研究および線量測定等である。

Contents

I. Introduction	1
II. Current Research Activities	3
1. Effects of Maleates and Solvent on the Formation of Tartaric Acid by XeF-laser Irradiation of Aqueous Maleic Acid-H ₂ O ₂ Solution	3
2. Photoreaction of 2-adamantanone via Higher Excited State	6
3. Improvement of Adhesive Property of Fluoropolymers with Ultraviolet Absorbent using Excimer Laser Irradiation	9
4. Improvement of Filterability of PTFE Membrane with Excimer Laser Irradiation	12
5. Surface Modification of Tetrafluoroethylene-perfluoroalkyl Vinyl Ether Copolymer by Excimer Laser Irradiation	15
6. Wavelength Dependence of Excimer Laser Irradiation Effects on Ethylene-tetrafluoroethylene Copolymer	18
7. Infrared Multiple-photon Decomposition of Si ₂ F ₆ with Irradiation of Pulsed CO ₂ Laser	21
8. The Effect of Excimer Laser Beams Irradiation on Fluoride Ion Uptake of Tooth Enamel	24
9. Influence of Excimer Laser Beams on Salivary α -amylase Activity (II)	28
10. Radiation-induced Polymerization of Spin-casted Epoxy Films	31
11. Growth and Sedimentation of Fine Particles Formed in Aqueous Solutions of Palladium Sulfate by Gamma-ray Irradiation	36
12. Formation of Palladium Clusters and Particles from Aqueous Solution of Sodium Chloro-palladate by Gamma-ray Irradiation	40
13. Photo-emission from Excited CO ₂ Ion by High Energy Electron Irradiation of Neon-carbon Dioxide Gas Mixture	44
14. Depth-dose Distributions in a Thin-layer Absorber Irradiated by 300 keV Electrons	48
15. Operation and Maintenance of Irradiation Facilities	54
III. List of Publications	55
1. Published Papers	55
2. Oral Presentations	56
3. Patent Applications	58

IV. List of Cooperative Studies	60
V. List of Personnel	61

I. Introduction

The annual research activities of Osaka Laboratory for Radiation Chemistry, Japan Atomic Energy Research Institute, during the period of April 1993 - March 1994, are presented in this report.

The research activities were conducted under the following two research programs:

Study on Laser-induced Organic Chemical Reactions, and

Study on Basic Radiation Technology for Functional Materials

with the support of Operation and Maintenance Group of the irradiation facilities. The total number of people working in the laboratory was 26 including visiting research collaborator from industrial companies and research students from universities. JAERI funded expenditures during the period amounted to about 110 million yen, excluding personnel expenses.

The study on laser-induced organic chemical reactions was initiated in 1988 as an advanced frontier subject to utilize lasers to chemistry. Under this program, studies were carried out on (1) laser-induced chemical transformation; selective formation of tartaric acid and decarboxylation of 2-adamantanone from higher excited singlet state, and (2) surface chemical reactions induced by excimer-laser irradiation of fluorine polymers; wavelength dependence of surface reactions of ethylene-tetrafluoroethylene copolymer. Based on the fundamental study of polymer-surface reactions, development studies of effective technic were extensively made for the improvements of adhesive property and wettability on the surfaces of some fluorine polymers.

Concerning the research program of the basic study on radiation technology for functional materials, studies were carried out on (1) polymerization of spin casted epoxy film to obtain thin insulating film and preparation of self-organized monomolecular film for future molecular functional device, (2) preparation of ultra-fine metallic particles having catalytic functions and (3) low energy electron beam dosimetry.

In the operation and maintenance of the irradiation facilities, the cobalt gamma ray source and the Van de Graaff accelerator of 2 MeV were operated without any serious trouble for the irradiation. However, the operation of an accelerator of rectifier transformer type of 800 keV had to be interrupted due to the electric insulation failure of a cable. A new oil filled cable was installed in the accelerator and some modification and improvement of the facility were made.

Cooperate research programs with universities were carried out with 9 groups, while joint research programs with industrial companies were carried out under 4 subjects.

Irradiation service has been extended to the request of the researchers outside of the laboratory since April 1991. This year, 20% of beam time was used for this purpose.

A training program which is offered for scientists and engineers from industries has been carried out once a year since 1968. This seven day program includes lectures and laboratory experiences concerned with the radiation chemistry of polymers. We accepted 14 trainees this year. A seminar was offered to local citizens to give them basic knowledge on nuclear power and radiation. About 80 citizens joined this one day seminar.

Detailed descriptions of the activities are given in Chapter 2. The list of the publications is given in Chapter 3, and the cooperative studies are summarized in Chapter 4.

Dr. Masafumi Nakano, Director
Osaka Laboratory for Radiation Chemistry

II. Current Research Activities

1. Effects of Maleates and Solvent on the Formation of Tartaric Acid by XeF-laser Irradiation of Aqueous Maleic Acid-H₂O₂ Solution

Y. Shimizu, S. Sugimoto* and S. Kawanishi

We are studying the laser-induced photochemical reaction of organic compounds in order to synthesize more valuable compounds directly and selectively from common organic resources. As a part of this study, we are conducting to synthesize hydroxy acid from aqueous organic acid solutions such as maleic acid containing hydrogen peroxide using an excimer laser with high intensity.

In the preceding annual report,¹⁾ we demonstrated that tartaric acid, which is able to possess optically active, is produced when the maleates such as disodium and calcium maleic acids aqueous solutions were irradiated by XeF laser in the presence of H₂O₂. We report here in further detail with regard to the laser-induced efficient synthesis of tartaric acid from aqueous various maleates-H₂O₂ solutions and also the effects of solvent such as 1,4-dioxane on the selective synthesis of tartaric acid.

The dipotassium maleate(2K) was prepared by adding excess potassium hydroxide to methanol solution of maleic acid(2H). The N₂-saturated aqueous solution of 2K(20 mM) was irradiated with the XeF laser(wavelength: 351 nm, pulse energy: 80 mJ/pulse, frequency: 16 Hz) at room temperature. An aqueous 30% H₂O₂ was added to the solution at feeding rate of 3.4 ml/h. Analysis of the products was carried out using ion chromatography(Yokogawa IC-100).

Table 1 shows the effects of various metals in maleates on the quantities of hydroxy acid. The XeF-laser irradiation of 2K aqueous solution increasingly enhanced the formation of tartaric acid. Thus, it was found that the quantity of tartaric acid increases in order of 2H, 2Na, Ca, and 2K. It is apparent that the order of the reactivity of the maleates on the formation of tartaric acid corresponds to that of ionization series²⁾ of the metals in maleates used. Also, the selectivity of tartaric acid formation with 2K was greatly increased from 4 for 2H to 19%. These results indicate that the stability of the monohydroxylated intermediate, which is formed by the addition of one hydroxyl radical generated from the laser-photolysis of H₂O₂ to the double bond of maleic acid, is very of importance for the efficient formation of tartaric acid.

* Radiation Application Development Association

For the purpose of further efficient synthesis of tartaric acid, we have attempted to induce efficiently the further addition of another hydroxyl radical to the monohydroxylated intermediate by irradiating 2H in 1,4-dioxane which has little the absorption in the wavelength around 351 nm, and has good solubility to 2H at R.T.

Figure 1 shows the quantities of main products as a function of irradiation time. The quantity of tartaric acid gradually increased with irradiation time, and was much greater than that of glycolic acid within about 25 min. The selectivity of tartaric acid formation was 76% at 10 min irradiation. Thus, it was found that tartaric acid is selectively produced by XeF-laser irradiation of maleic acid containing H₂O₂ in 1,4-dioxane.

References

- 1) Y. Shimizu, S. Kawanishi, M. Nishii, S. Sugimoto, and N. Suzuki, JAERI-M 94-017, 3(1994).
- 2) "Rika-gaku Jiten," ed by R. Kubo, S. Nagakura, H. Iguchi, and H. Ezawa, Iwanami Shoten, Tokyo (1987), pp.64.

Table 1 The effect of maleates

Hydroxy acid ^{a)}	Maleate				
	2K	Ca	2Na	Na·H	2H
Tartaric acid	1.7	1.5	1.4	0.4	0.4
Malic acid	1.1	1.0	0.9	0.6	0.4

a) Unit:mM, Irradiation time:45 min, H_2O_2 :3.4ml h^{-1} .

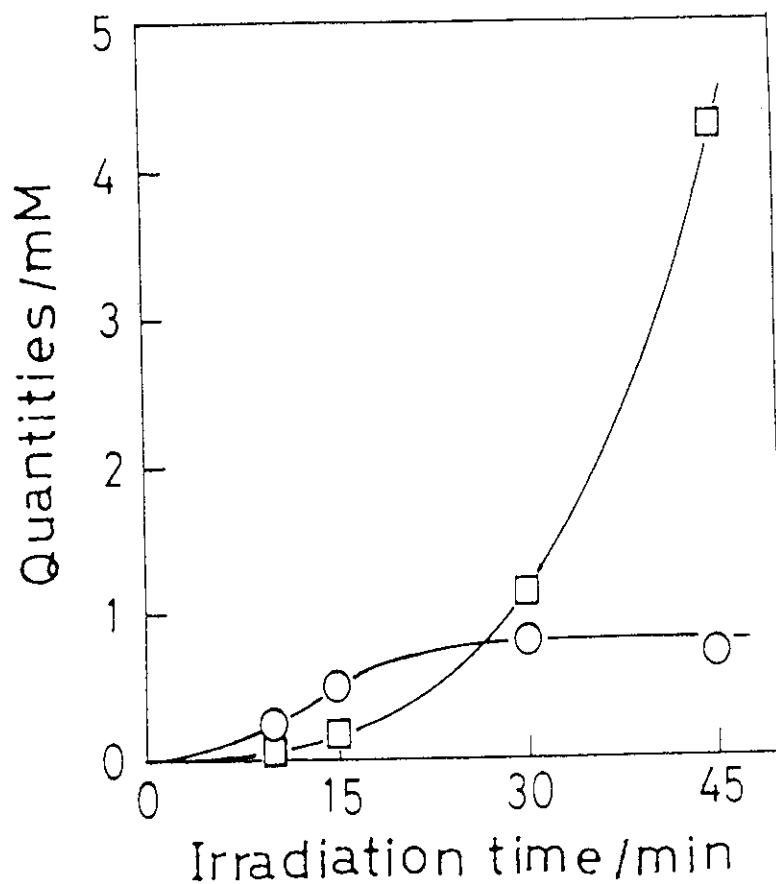


Fig.1 Relationship between the quantities of tartaric (○) and glycolic (□) acids with irradiation time upon laser irradiation of 2H maleate- H_2O_2 solution in 1,4-dioxane. H_2O_2 : 3.2 ml h^{-1} .

2. Photoreaction of 2-Adamantanone via Higher Excited State

N. Ichinose and S. Kawanishi

Excimer lasers have been used widely as a light source for preparative laser-induced photoreactions. Multi-photon excitation process will be a typical feature of primary process upon irradiation of intense laser light to organic compounds. Higher excited singlet and triplet states (S_n and T_n states) as well as the lowest excited singlet and triplet states (S_1 and T_1 states) may be produced within the pulse (10 - 30 ns) of excimer lasers. Generally, these species are believed to decay promptly to the S_1 and T_1 states. Some organic compounds, however, undergo chemical reactions via higher excited states. We now report a chemical behavior of 2-adamantanone upon intense laser irradiation in solution.¹⁾

2-Adamantanone (1) shows a typical UV-absorption of aliphatic ketone, which have a maximum at 288 nm ($\epsilon = 19 \text{ M}^{-1} \text{ cm}^{-1}$) in cyclohexane corresponding to n, π^* transition. Though aliphatic ketones generally undergo various photoreactions such as Norrish Type I and II reactions, 1 is exceptionally stable toward photoexcitation to the n, π^* S_1 and T_1 states.²⁾ A cyclohexane solution of 1 (4 mL; 4×10^{-2} M) containing adamantane (2×10^{-2} M) as an internal standard was irradiated for 24 h at 254 nm with a 60-W low-pressure mercury lamp. The solution was analyzed by gas chromatography (GC) to indicate complete recovery of 1. On the other hand, 64% of 1 was consumed by the irradiation of a 30-mL portion of its cyclohexane solution with a XeCl laser (308 nm, $110 \text{ mJ cm}^{-2} \text{ pulse}^{-1}$, repetition rate of 10 Hz) for 5 h. The reaction mixture was submitted to column chromatography on silica gel with hexane to give noradamantane (tricyclo[3.3.1.0^{3,7}]nonane) (2) in a 42% isolated yield. GC and GC-MS analyses revealed that small amount of 2-adamantanol (3) (<5%) was also formed. Apparently, 2 was formed by the loss of CO group. Similar irradiation of 1 afforded 2 and 3 together with 2,2-dimethoxyadamantane (4) and 2-hydroxy-2-hydroxymethyladamantane (5).

Laser intensity dependence of the consumption of 1 and formation of 2 was examined for the range of 40 - 160 $\text{mJ cm}^{-2} \text{ pulse}^{-1}$. Figure 1 shows the relationship of the initial consumption of 1 and formation of 2 per 1000 pulses (conversion < 25%) in cyclohexane versus laser intensity. The slope of the intensity dependence was 2 to indicate that the photoreaction of 1 proceeded via two-photon excitation. Similar results were also obtained for the photoreaction in methanol. The formation of 2 was not affected by the addition of biphenyl, a triplet quencher for aliphatic

ketones with lower triplet energy (E_T) than 2 ($E_T = 65 \text{ kcal mol}^{-1}$; $E_T = 79 \text{ kcal mol}^{-1}$ for aliphatic ketones).³⁾ This rules out the further excitation of T_1 state of 1 within the laser pulse. The lifetime of the S_1 state of 1 (9 ns)⁴⁾ comparable with the pulse width (8 - 12 ns) also rules out the excitation of T_1 in the formation of 2.

Two photon energy at 308 nm is larger than photon energy of 185-nm light from super low-pressure mercury lamp, where 1 has another absorption band. Irradiation of 1 in cyclohexane at 185 nm gave 2 and 3. This supports the incorporation of higher excited singlet state of 1 as a key intermediate in the present laser-induced photoreaction of 1, though it is not clear whether the simultaneous or step-wise two-photon excitation mechanism works.

Present study has demonstrated a photoreaction of an aliphatic ketone via higher excited state formed by the two-photon process or direct excitation with a vacuum UV-light. This strongly suggests a potential reactivity of higher excited states of other organic molecules upon intense laser irradiation.

References

- 1) Preliminary report: N. Ichinose and S. Kawanishi, *J. Chem. Soc., Chem. Commun.*, 1994, 2017.
- 2) T. Sasaki, S. Eguchi, and M. Mizutani, *Synth. Commun.*, 3, 369(1973).
- 3) S.L. Murov, I. Carmichael, and G.L. Hug, "Handbook of Photochemistry 2nd Ed.," Marcel Dekker: New York, 1992.
- 4) D.R. Charney, J.C. Dalton, R.R. Hautala, J.J. Snyder, and N.J. Turro, *J. Am. Chem. Soc.*, 96, 1407(1974).

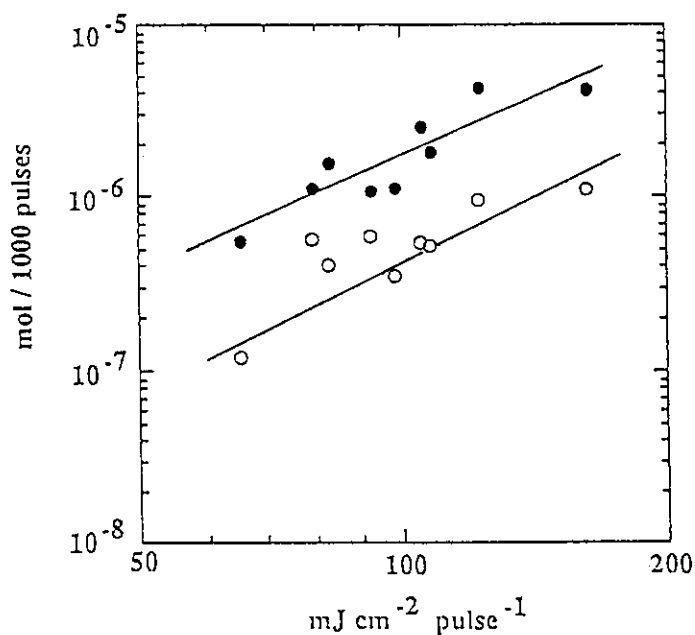
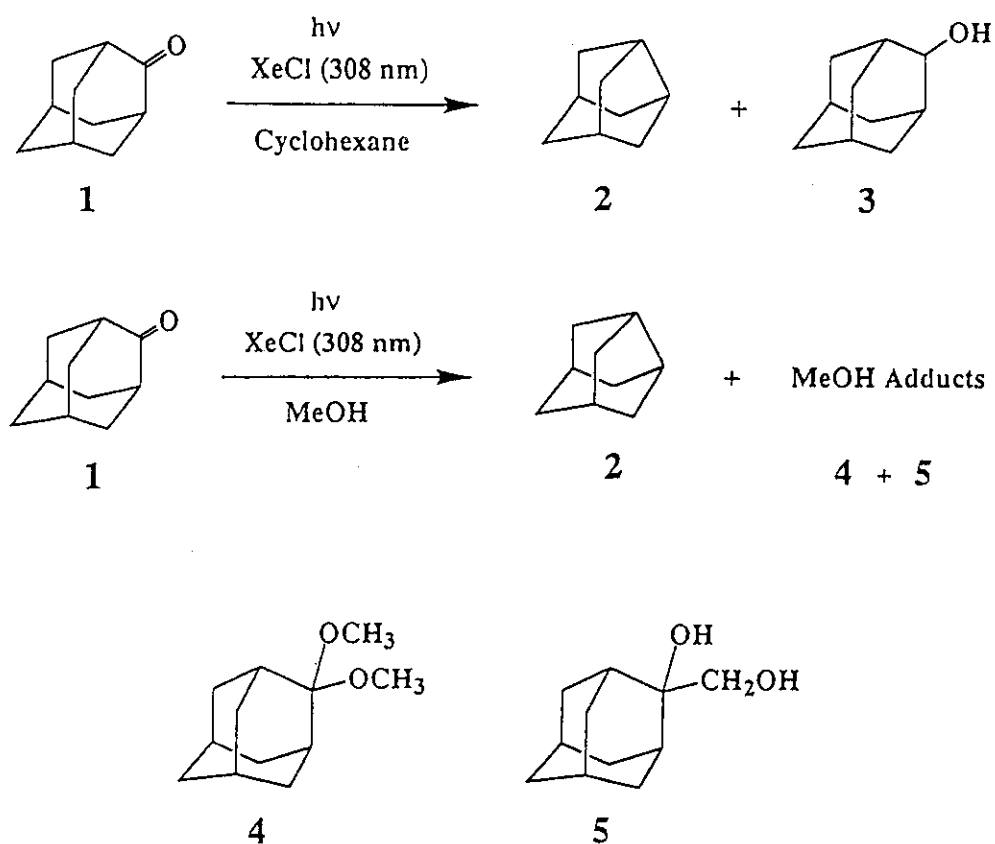


Fig. 1 Initial conversion of 1 (closed circle) and formation of 2 (open circle) in cyclohexane versus intensity of XeCl laser pulse: $[1] = 4 \times 10^{-2}$ M

3. Improvement of Adhesive Property of Fluoropolymers with Ultraviolet Absorbent using Excimer Laser Irradiation

T. Nagase*, M. Endo*, M. Nishii, S. Sugimoto**, and S. Kawanishi

Fluoropolymers have excellent properties such as thermal stability and chemical inertness, but adhesive property is entirely poor. We have attempted to improve adhesive property of fluoropolymers by excimer laser irradiation.

100- μm -thick tetrafluoroethylene-perfluoroalkylvinylether copolymer (PFA) and tetrafluoroethylene-hexafluoropropylene copolymer (FEP) films were used as sample. PFA and FEP have no absorption band in ultraviolet region. In this report aqueous sodium benzoate solution was coated as ultraviolet absorbent in order that films may absorb ultraviolet light. Surfactant containing perfluoroalkyl group was added to the aqueous solution in order to reduce surface tension. This solution can be coated uniformly by an applicator (thickness: 25 μm). After drying, the film was irradiated with KrF laser radiation (wavelength: 248nm, fluence: 150-300 $\text{mJ cm}^{-2} \text{ pulse}^{-1}$, frequency: 40Hz, number of pulses: 2-10) in air at room temperature. The adhesive strength of the irradiated film was evaluated by the measurement of the 180° peel strength adhered on a stainless steel plate with the epoxy resin adhesive. Surface morphology of irradiated film was observed by SEM and chemical structure was analyzed by XPS.

The adhesive property of PFA and FEP films were not improved at all without coating ultraviolet absorbent by KrF laser irradiation (fluence: 300 $\text{mJ cm}^{-2} \text{ pulse}^{-1}$, irradiation energy: 3.0 J cm^{-2}). When the film coated with sodium benzoate as ultraviolet absorbent, the adhesive strength was remarkably enhanced. Figure 1 shows the peel strength of PFA irradiated by KrF laser in various fluence. The 180° peel strength of PFA film became 1.4 kg cm^{-1} by KrF laser irradiation (fluence: 300 $\text{mJ cm}^{-2} \text{ pulse}^{-1}$, irradiation energy: 0.6 J cm^{-2}) from less than 0.01 kg cm^{-1} of untreated film. As shown in Fig.1 the reaction induced by excimer laser is dependent on the laser fluence with the threshold of 150-200 $\text{mJ cm}^{-2} \text{ pulse}^{-1}$. The peel strength of FEP film became 1.0 kg cm^{-1} by KrF irradiation (fluence: 300 $\text{mJ cm}^{-2} \text{ pulse}^{-1}$, irradiation energy: 0.6 J cm^{-2}). The peel strength of FEP film almost changed as the same as PFA film.

XPS spectrum of irradiated PFA film indicated decrease of fluorine atom and increase of oxygen atom. With irradiation of 0.6 J cm^{-2} , F/C ratio became 0.68 from 2.10, and

* Technical Research Laboratory, Kurabo Industries, Ltd.

** Radiation Application Development Association

O/C ratio became 0.14 from 0.01. Figure 2 shows that relationship between the peel strength and O/C ratio of PFA. The peel strength linearly increased with O/C ratio. From this result, polar group with oxidation takes an important role to enhance adhesive property. As irradiation energy increased polar group was decomposed and the peel strength reduced. SEM image of irradiated film indicated that morphology of film was not changed by laser irradiation. From these evidences, it is presumed that the change of chemical structure mainly induce the improvement of adhesive property.

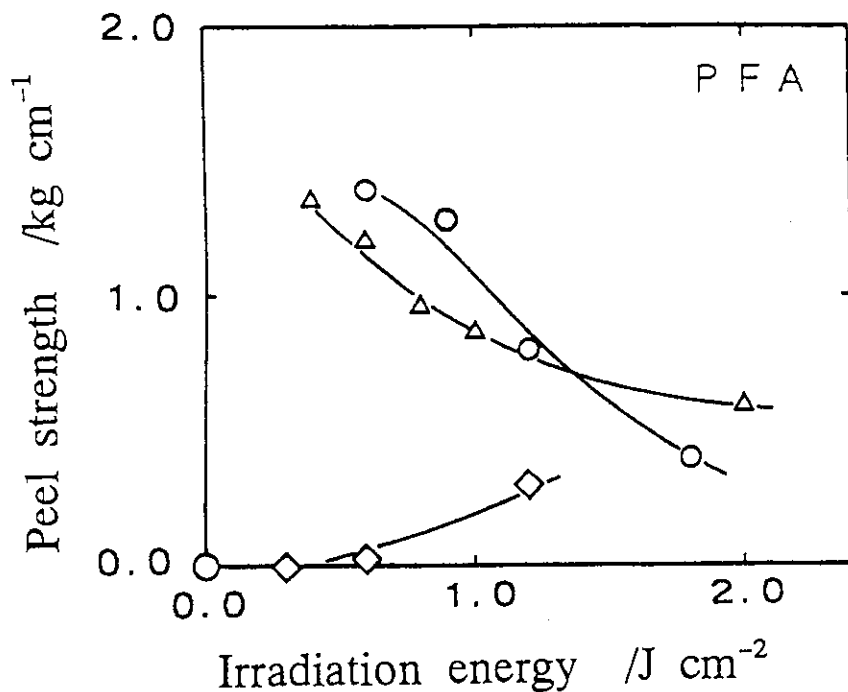


Fig.1 Peel strength of the PFA films coated with aqueous sodium benzoate solution irradiated by KrF laser.

- (○) Fluence 300 mJ cm⁻² pulse⁻¹
- (△) 200 mJ cm⁻² pulse⁻¹
- (◇) 150 mJ cm⁻² pulse⁻¹

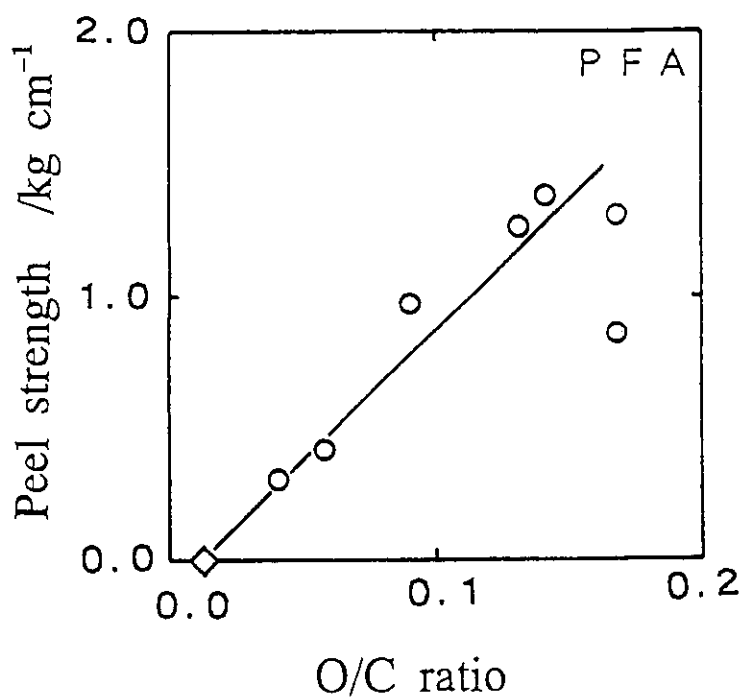


Fig.2 Relationship between O/C ratio of PFA and peel strength.

- Fluence 300 mJ cm⁻² pulse⁻¹,
- (◇) Untreated PFA
- (○) Sodium benzoate water solution.

4. Improvement of Filterability of PTFE Membrane with Excimer Laser Irradiation

T. Tanaka*, M. Sano*, M. Nishii, S. Sugimoto**, and S. Kawanishi

PTFE membrane have superior properties such as thermal and chemical resistance in comparison with other membranes, but poor in wettability. It is difficult to filter the chemicals that have high surface tension or the aqueous chemicals directly with PTFE membrane. Therefore, we have attempted to give wettability for the PTFE membrane, and have reported in previous report that wettability of the PTFE membrane can be improved when it was impregnated with sodium silicate aqueous solution and was irradiated KrF or ArF excimer laser afloat on sodium silicate aqueous solution at room temperature. In this study, the effect when hydrogen peroxide aqueous solution are impregnated the PTFE membrane was investigated. And the filterability of the cartridge which was composed of the treated membrane was evaluated.

The PTFE membrane was obtained from Japan Goretex. A pore size and a thickness of PTFE membrane were $0.1\ \mu\text{m}$ and $45\ \mu\text{m}$, respectively. The membrane was impregnated with hydrogen peroxide aqueous solution, and was irradiated with KrF or ArF excimer laser from the upper side afloat on the hydrogen peroxide aqueous solution at room temperature. The treated membrane was sufficiently washed with pure water, then dried. Wettability of treated membrane was evaluated by the measurement of the wettability index using the standard solutions prepared according to JIS K-6768 specification. The standard solutions were dropped on the membrane in ascending order of the surface tensions. The wettability index of the membrane was determined as the maximum surface tension of the standard solution which wets the membrane. With this method, the wettability index of a pristine was less than $31\ \text{dyn cm}^{-1}$.

Wettability of the membrane when it was impregnated with hydrogen peroxide aqueous solution was improved remarkably by KrF or ArF excimer laser irradiation. Figure 1 shows the relationship between the energy of laser and the wettability index of PTFE membrane. The wettability index of the treated membrane increased with the energy of laser. The wettability index of the membrane irradiated by KrF excimer laser (fluence: $200\ \text{mJ cm}^{-2}\ \text{pulse}^{-1}$, energy: $10\ \text{J cm}^{-2}$) was $35\ \text{dyn cm}^{-1}$ and the wettability index of membrane irradiated by ArF excimer laser (fluence: $20\ \text{mJ cm}^{-2}\ \text{pulse}^{-1}$, energy: $10\ \text{J cm}^{-2}$) was modified up $48\ \text{dyn cm}^{-1}$. Enhancement of the wetting properties of the

* Technical Research Laboratory, Kurabo Industries, Ltd.

** Radiation Application Development Association

membrane irradiated by ArF excimer laser become more remarkable than that of KrF excimer laser. On the other hand, when it was not impregnated with hydrogen peroxide aqueous solution, the index of the membrane irradiated in the same condition was less than 31 dyn cm^{-1} .

The X-ray photoelectron spectroscopic analysis of the treated membrane showed a formation of polar carboxyl group on the surface thereof. And the electron microscopic observation indicated no structural change of the treated membrane. From these results, it is considered that this modification is not due to the morphological change, but due to the change of chemical structure.

Figure 2 shows the flux of 40wt% ammonium fluoride aqueous solution whose surface tension is 92 dyn cm^{-1} (differential pressure, $\Delta P = 0.5 \text{ kg cm}^{-2}$, 25°C), as a function of the time. The cartridge composed of the treated membrane has high flux from the start and stable as the time passage. On the other hand, the cartridge composed of the untreated membrane has no flux from the start. From these results, it was able to filter the high surface tension chemicals with ease and to filter many chemicals directly by the PTFE membrane improved of wettability. This method with excimer laser irradiation can modify any part of the PTFE material in wettability, therefore it is expected for the application to medical facilities and electronic industry and so on.

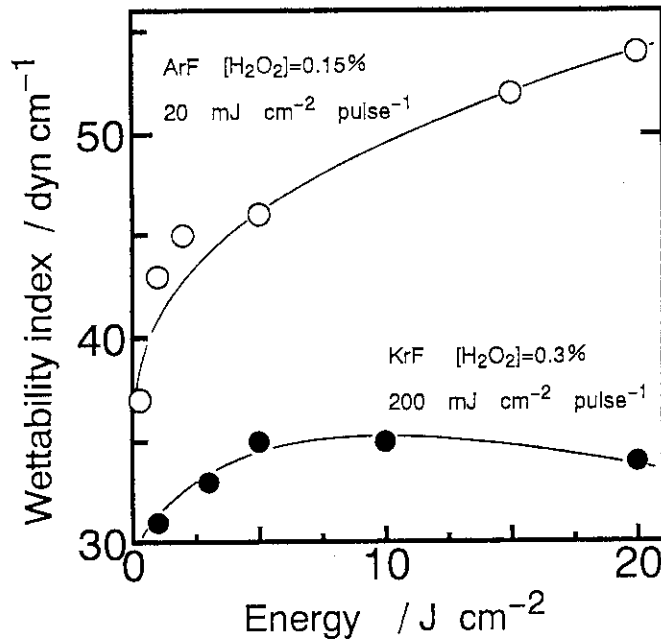


Fig.1 Wettability index of PTFE membrane irradiated by ArF or KrF excimer laser.

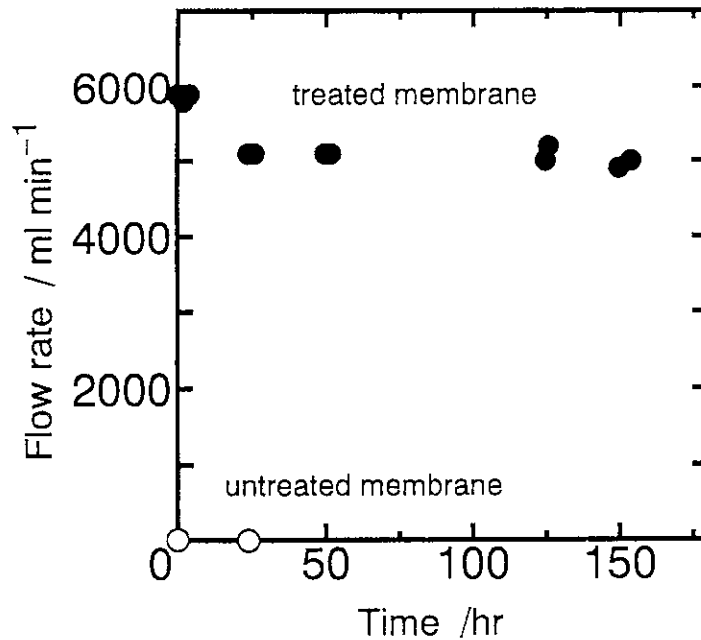


Fig.2 NH₄F flux of PTFE membrane irradiated with ArF excimer laser.
Differential pressure: 0.5 kg cm⁻²
Concentration of NH₄F: 40 wt%

5. Surface Modification of Tetrafluoroethylene-perfluoroalkyl Vinyl Ether Copolymer by Excimer Laser Irradiation

A. Okada* , Y. Negishi*, Y. Shimizu, S. Sugimoto**, and S. Kawanishi

In the previous report,¹⁾ we have proposed that the endowment with the wettability on the surface of tetrafluoroethylene-perfluoroalkyl vinyl ether copolymer (PFA) by excimer laser irradiation in water saturated with carbon monoxide (CO). In this study, we have examined the effects of rare gases dissolved in water on the ArF-laser induced surface modification of PFA for practical purposes such as efficiency, safety and handling.

PFA films (0.1 mm thickness) were prepared from the extrusion processing, and were washed with ethanol before irradiation. The PFA film was irradiated with an ArF laser (fluence: $13 \text{ mJ cm}^{-2} \text{ pulse}^{-1}$, frequency: 50 Hz, number of pulses: 16000 pulse, beam size: $16.7 \times 8.0 \text{ mm}$) at room temperature in distilled water saturated with rare gases (He, Ne, Ar, and Xe) by bubbling for 15 min. The wettability of the PFA film was evaluated from the contact angle with water at room temperature. The surface of the PFA film was analyzed by X-ray photoelectron spectroscopy (XPS).

The results are summarized in Table 1 together with the saturated concentration of each gas.²⁾ The contact angle of the original PFA film was 106 degrees, and that of irradiated one in air without water was 100 degrees. The contact angle was decreased remarkably to 45 degrees by the ArF-laser irradiation in the Ar-saturated water. The similar irradiation in water saturated with He or Ne was also effective as compared to that with O_2 . It was revealed that the rare gases as well as water play an important role for the endowment with the wettability on the surface of the PFA film.

In the case of the ArF-laser irradiation in the Ar-saturated water, five peaks at 285.5 - 292 eV appeared in the XPS spectra of the PFA film in C1s region together with two original peaks at 285.5 eV (-C-C-) and 294 eV (-CF₂-), which were assigned to -C=C-, -C-O, C=O, -COO-, and -CF- in the order of binding energy, respectively. Furthermore, the peak area of the O1s signal was increased, whereas that of the F1s XPS was decreased by the ArF-laser irradiation. These results indicate replacement of the fluorine atom with oxygen, and formation of C=C double bond at the surface as reported in the previous study with CO.¹⁾ Figure 1 shows a correlation between the atomic ratios (F/C, O/C) and the contact angle of the surface with water. It demonstrates that the

* Shiga Laboratory, Gunze Ltd.

** Radiation Application Development Association

results obtained for rare gases are in good accordance with those for CO. It is therefore concluded that the irradiations in rare gases and CO-saturated water will cause the same chemical reaction toward the PFA film surface.

In the present photoreaction, water acts essentially to the reaction as an oxygen source for the formation of polar groups such as -OH or -COOH, and the rare gases act indirectly in expelling oxygen, a scavenger for both excited and radical species. The present ArF-laser induced photoreaction is a useful method for preparing functionalized surface on fluoropolymer and is to be studied further as well as its mechanistic feature.

References

- 1) A. Okada, Y. Negishi, Y. Shimizu, S. Sugimoto, N. Nishii, and S. Kawanishi, *Chem. Lett.*, 1993, 1637.
- 2) "Kagaku Binran, Kiso," ed. by The Chemical Society of Japan, Maruzen, Tokyo (1984), Part II, p.158.

Table 1 Contact angles of the PFA films irradiated with ArF-laser pulses

condition	saturated concentration in water at 20°C/wt%	contact angle/deg.
original	—	105.7
in air	—	100.0
in water saturated with		
carbon monoxide	3.1×10^{-3}	53.0
oxygen	4.8×10^{-3}	102.0
helium	1.7×10^{-4}	54.9
neon	1.0×10^{-3}	46.1
argon	6.5×10^{-3}	45.3
xenon	6.9×10^{-2}	62.5

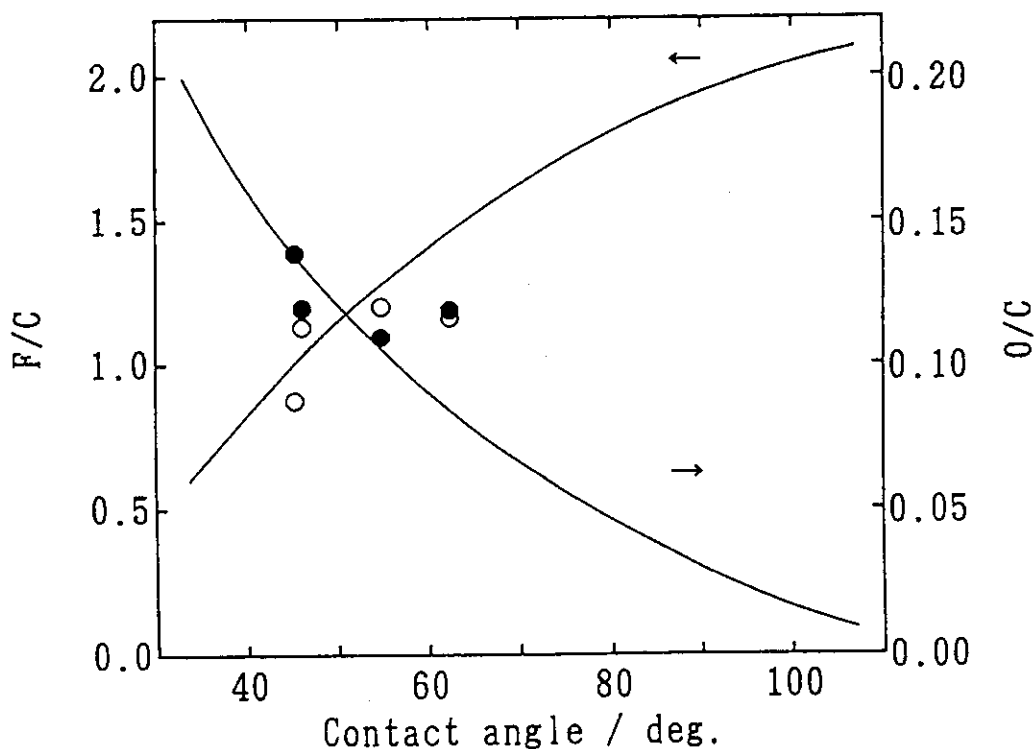


Fig.1 Relationship between contact angle and ratios of atomic concentrations. (—) results of carbon monoxide, (○) F/C of rare gases, (●) O/C of rare gases.

6. Wavelength Dependence of Excimer Laser Irradiation Effects on Ethylene-tetrafluoroethylene Copolymer

Y. Hamada*, S. Kawanishi, M. Nishii, S. Sugimoto**, and T. Yamamoto*

Very few reports concerned with wavelength dependence of the interaction of the excimer laser with fluoropolymers. In this study we picked up an ethylene-tetrafluoroethylene copolymer (ETFE) from various fluoropolymers because ETFE has higher absorbance in the ultraviolet and visible (UV-vis) region than others, which enabled us to study the excimer laser irradiation effects on fluoropolymers without reactive additions. Using an UV-vis spectroscopy we studied a wavelength dependence of the chemical changes of ETFE irradiated with ArF(193 nm), KrF(248 nm) and XeCl(308 nm) lasers in vacuum or in air for the purpose of informing how the modification of the fluoropolymers was performed.

The ETFE used in this study was 100 μm thick film. Before the experiments the film was cleaned with ethanol using a supersonic wave for 10 min. The ETFE film was irradiated with ArF, KrF and XeCl excimer lasers (Lumonics Hyper EX-460). The laser irradiation was carried out at room temperature, and the frequency for operating laser was kept below 5 Hz in order to avoid possible effects arising from heating of the sample.

UV-vis differential spectra between unirradiated ETFE and ETFE irradiated in vacuum and in air are shown in Fig. 1, where the change in absorbance is plotted against wavelength. The influence of the reflectance on the differential spectrum can be negligible. The photon energy absorbed in the ETFE film were 8.0, 7.3 and 7.5 $\text{J} \cdot \text{cm}^{-2}$ for 193, 248 and 308 nm radiations, respectively. For avoiding the effects of the wavelength variation in the absorption coefficient, which is necessary to investigate the wavelength dependence, the value of the energy absorbed into the ETFE film has been made consistent for each wavelength radiation instead of the incident energy.

Figure 1 (a) shows that an absorption band at the wavelength of about 230 nm dominates the differential spectrum after ArF-laser (193 nm) irradiation in vacuum and in air. This absorption band is suggested to attribute to the $\pi \rightarrow \pi^*$ transition of diene ($-\text{C}=\text{C}-\text{C}=\text{C}-$) because the absorption band disappeared after bromination similar to the result of the brominated PVdF.¹⁾

* Osaka University

** Radiation Application Development Association

Figure 1 (b) shows that KrF laser (248 nm) radiation caused the increase in the absorbance in the full range of the wavelength measured, 190-500 nm, with the film being blackened. The increase in absorbance is considered to be due to amorphous carbon with the bond scission in the structure of ETFE. The more increase in absorbance after radiation in air than that in vacuum indicates that oxygen in air accelerated the carbonization of ETFE irradiated at 248 nm similar to the result of the laser ablation of PMMA.²⁾ As can be seen in Fig.1(c), the chemical changes in ETFE induced by XeCl laser (308 nm) irradiation appears to be similar to those induced by 248 nm irradiation. Therefore, 308 nm radiation is considered to bring about the same reaction as that with 248 nm radiation.

The change in absorbance at wavelength of 230 nm induced by ArF-laser irradiation(\circ), which expresses the quantity of diene formed in the bulk of ETFE, is plotted as a function of the laser fluence in Fig.2, and those at wavelength of 500 nm induced by KrF(\triangle), XeCl-laser(\blacksquare) irradiation, which expresses those of the amorphous carbon, are plotted in the same figure. These plots bear linear relations for all wavelength radiation, and the values of their slopes are 1.0, 3.6 and 4.4 for ArF laser (193 nm), KrF laser (248 nm) and XeCl laser (308 nm), respectively. Then with 193 nm radiation on ETFE diene is found to be formed through the process of single-photon absorption, because the value of n is 1.0. At 248 and 308 nm the values of 3.6 and 4.4 indicates that the carbonization of ETFE was led through the process of multiphoton absorption. The difference of radiation effect at 193 nm from those at longer wavelengths can be ascribed into whether laser-induced reaction is single-photon process or multiphoton process. Moreover, scanning electron micrographs shows no heating effects on the surface of ETFE at 193 nm radiation, while at 248 and 308 nm radiation made the surface melted. It is supposed from these phenomena that photochemical bond breaking played an important role at 193 nm,³⁻⁵⁾ photothermal local heating with multiphoton process made ETFE carbonized at 248 and 308 nm. Multiphoton of 248 and 308 nm may be absorbed through the process of $T \rightarrow T^*$ transition with an evolution of heat.⁶⁾

References

- 1) J.H. Brannon, J.R. Lankard, A.I. Baise, F. Burns, and J. Kaufman, *J. Appl. Phys.* 58, 2036 (1985).
- 2) R. Sauerbrey and G.H. Pettit, *Appl. Phys. Lett.*, 55, 421 (1989).
- 3) G.M. Davis and M.C. Gower, *Appl. Phys. Lett.*, 50, 1286 (1987).
- 4) A.J. Dias and T.J. McCarthy, *Macromolecules*, 17, 2529 (1984).
- 5) N. Shimo, T. Uchida, and H. Masuhara, *Mat. Res. Soc. Symp. Proc.*, 191, 91 (1990).

6) H. Fukumura and H. Masuhara, *J. Photopolym. Sci. Technol.*, **5**, 223 (1992).

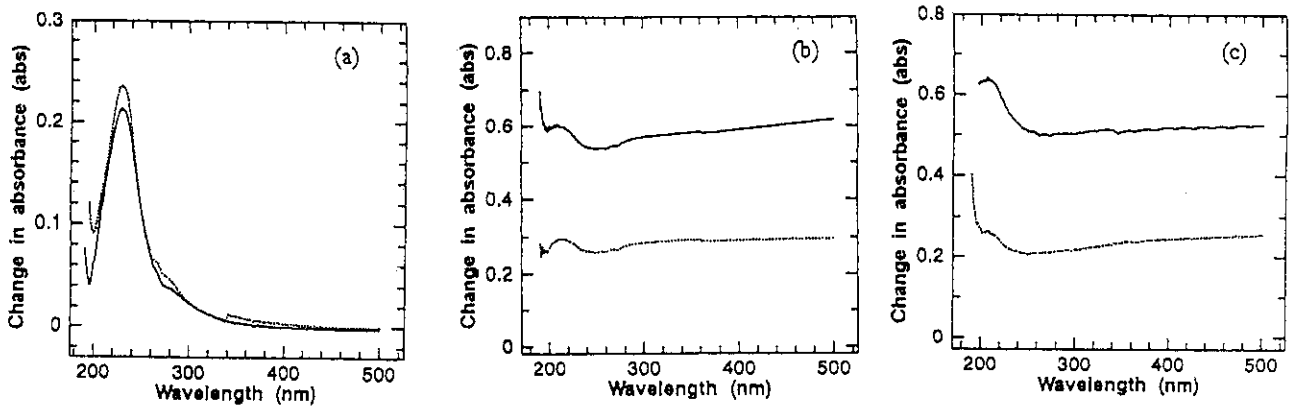


Fig. 1 Differential UV-vis absorption spectra between original ETFE and ETFE irradiated in air (straight line) or in vacuum (dashed line). (a) ArF-laser (193 nm) irradiation with $7.97 \text{ J} \cdot \text{cm}^{-2}$, (b) KrF-laser (248 nm) irradiation with $7.28 \text{ J} \cdot \text{cm}^{-2}$, (c) XeCl-laser (308 nm) irradiation with $7.50 \text{ J} \cdot \text{cm}^{-2}$.

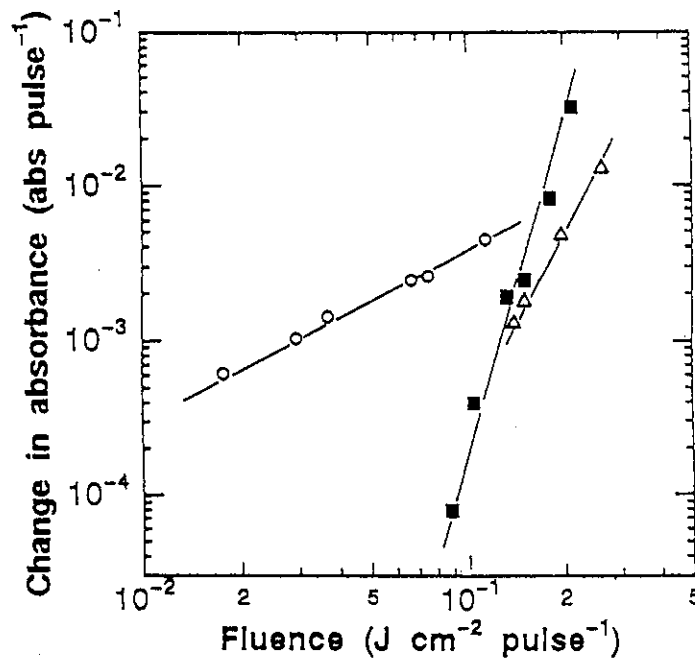


Fig. 2 Change in absorbance at 228 nm for ArF-laser (193 nm) irradiation (\circ), at 500 nm for KrF-laser (248 nm) irradiation (\triangle), and at 500 nm for XeCl-laser (308 nm) irradiation (\blacksquare) as a function of laser fluence.

7. Infrared Multiple-photon Decomposition of Si_2F_6 with Irradiation of Pulsed CO_2 Laser

S. Nakahashi*, S. Arai*, S. Sugimoto**, Y. Shimizu, and S. Kawanishi

It is well-known that infrared multiple-photon decomposition (IRMPD) shows remarkably large isotope effects under optimized irradiation condition.^{1, 2)} Therefore, considerable efforts have been towards its application to practical isotope separation and in order to elucidate its fundamental mechanism, Hexafluorodisilane Si_2F_6 is known to decompose into SiF_4 and SiF_2 radical through IRMPD with pulsed CO_2 laser irradiation. SiF_2 radical aggregates to form white powders. This reaction shows the large isotope effects and can be utilized in silicon isotope separation. In this study, we have studied the IRMPD of natural Si_2F_6 and clarified the relationships between laser fluence and decomposition properties with comparison of experimental results and calculation.

Natural Si_2F_6 gas was introduced to the reaction cell (volume 265 cm^3 , length 12 cm) with 0.05 torr and irradiated by the CO_2 TEA laser operated at the repetition rate of 0.2 Hz. The intensity of laser power was measured by a calory meter. Irradiation was carried out until the reaction yield of SiF_4 became about 10-20%. The analysis of SiF_4 was carried out using a gas chromatograph Shimadzu GC-9A.

For the simulation of the IRMPD process, at first we calculated the decomposition rate constant using RRKM theory. And using the decomposition rate constant, the distribution of energy levels and number of decomposed molecules by Monte Carlo method with a personal computer.

An absorption peak of Si_2F_6 of ground state was at 990cm^{-1} , which is due to Si-F stretching, however as shown in Fig.1, the wavenumber that is most effective for the IRMPD shifts to lower energy. This shows that the energy gap of the high vibrational levels are shorter than that of the ground and first vibrational states. The absorption cross section varies at each vibrational level. We assumed that the cross section of the first vibrational level is 1.5 times as that of the ground level, and those of higher levels gradually decrease with higher excitation.

In Fig.2, the comparison of the decomposition rates obtained with experiment and calculation was shown. These values were out of accord with each other. This result indicates the molecular collision takes an important role in the IRMPD process of Si_2F_6 .

* Material Science and Technology, Kyoto Institute of Technology

** Radiation Application Development Association

References

- 1) V. S. Letokhov, Phys. Today, May (1977) 23.
- 2) V. S. Letokhov, "Nonlinear Laser Chemistry, Springer, 1988".

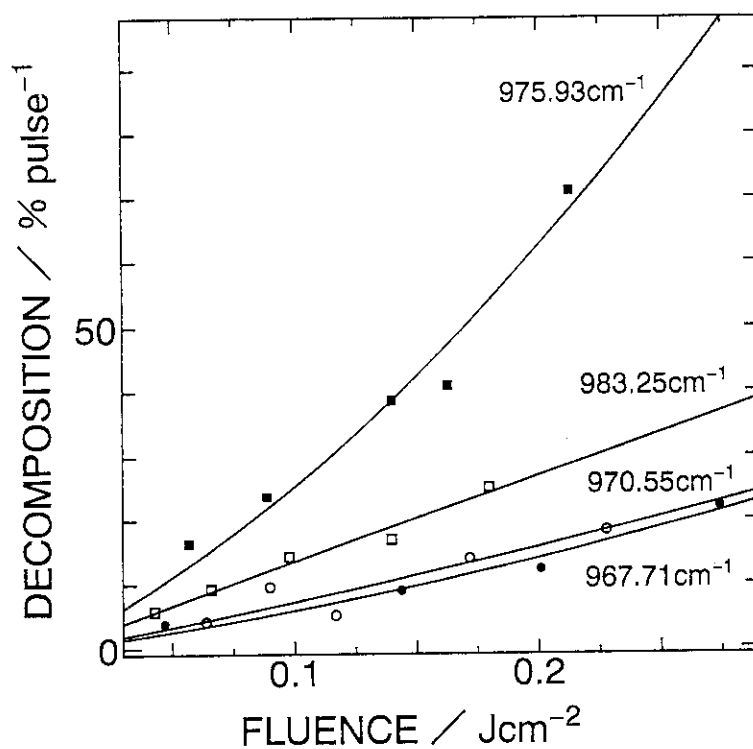


Fig.1 Decomposition probability vs laser fluence. (experimental data)

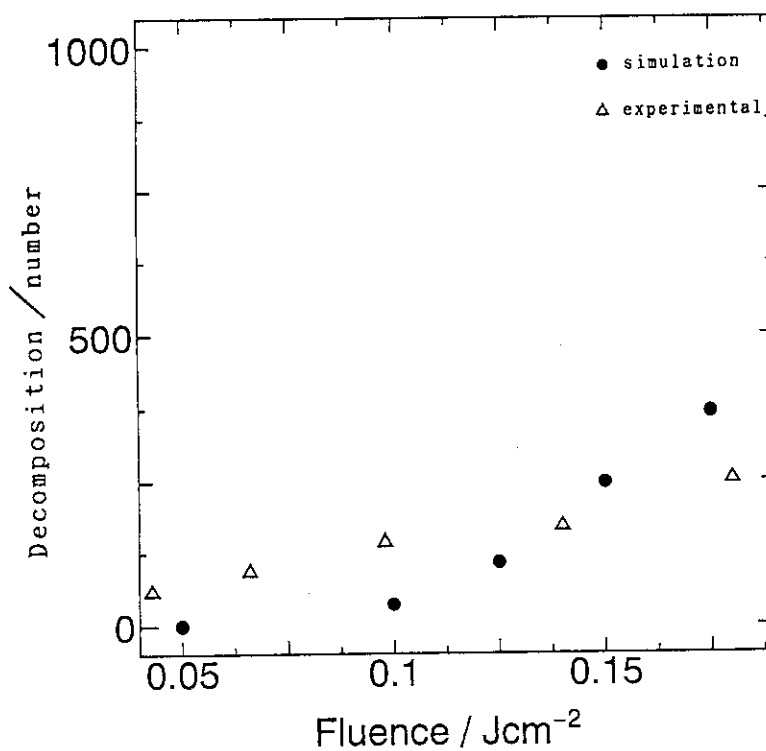


Fig.2 Comparison between experimental data and simulation. Laser wave number: 983.25 cm⁻¹

8. The Effect of Excimer Laser Beams Irradiation on Fluoride Ion Uptake of Tooth Enamel

C. Miyazawa*, S. Hamada*, M. Kokubun*, M. Amano*, T. Shimizu*, S. Sugimoto**,
Y. Shimizu, and S. Kawanishi

The hydroxyapatite (HAp) of enamel is susceptible to dental caries depending upon a high acid solubility. Fluoroapatite (FAP) can be produced upon tooth enamel under certain conditions. The FAP is produced by displacement of the HAp (OH^-) with fluoride (F^-). Enamel coated with FAP would be capable of preventing caries due to a strong acid resistance. Fluoride solution is routinely used as fluoride mouthrinsing or topical fluoride application in an effort to produce FAP. However, fluoride must be used for an extended period to produce enamel coated with FAP. The authors investigated the effect of excimer laser irradiation on enamel to produce improved, rapid and efficient fluoridization.¹⁾

This study used labial maxillary anterior permanent teeth and 200-300 μm of enamel powder extracted from completely erupted teeth.^{2, 3)} The labial maxillary anterior teeth and enamel powder were irradiated with KrF excimer laser (248 nm, Lumonics EX 884). Three different types of irradiation methods were used to study the effect of the laser beams upon the teeth and enamel powder. The first method of the irradiation (I) is fluence: 70 mJ/cm^2 and 1000 shot. The second method of the irradiation (II) is fluence: 70 mJ/cm^2 , 1430 shot. The third method of the irradiation (III) is fluence: 70 mJ/cm^2 , 1200 shot. The irradiated teeth were then placed into 100 $\text{m}\ell$ and 100 ppm F^- solution (NaF, $\text{pH } 7.0 \pm 0.1$). NaF solution 10 $\text{m}\ell$ /100 mg of enamel powder was added for 28 days. The solution was replaced with fresh NaF solution twice weekly. The labial surface of the anterior teeth was observed with a scanning electron microscope (Nihon Denshi, JSM 5300) with 10 kv of accelerating voltage. The teeth received a 100 \AA coating of Au and were examined at $\times 1000$ magnification. The CO_3^{2-} concentration of the teeth was quantitated by Conway's diffusion method. The enamel was washed with 1M-KOH. The FAP F^- and total F^- were then fractionally quantitated. The concentration of F^- was determined using an ion electrode (Orion Ionalyzer 901) according to McCann's Method. A mean value was determined by t-test.

Figure 1 shows the SEM findings of irradiation and fluoridated enamel. The irradiation of the enamel caused ablation of the enamel surface. The ablation of the enamel from

* Department of Preventive Dentistry, Ohu University

** Radiation Application Development Association

irradiation I produced a marked coarse enamel surface. A decrease of the coarse enamel surface was produced with stronger irradiation of II. The fluoridated enamel surfaces after irradiation I and II was almost smooth.^{2, 3)}

Figure 2 shows the F^- uptake of the fluoridated enamel. F^- uptake of total fluorine and FAp after irradiation II significantly increased to 9.1% of the former and 7.4% of the latter. This was more than the non-irradiation group. The F^- uptake may occur as a chemical reaction between a solid and a liquid on the surface of the enamel. The F^- value was elevated on the enamel surface.

The CO_3^{2-} concentration of the enamel irradiation with the excimer laser tends to decrease when compared the non-irradiated enamel. The irradiation II produced a significant reduction of the CO_3^{2-} concentration (Fig. 3).

The low CO_3^{2-} concentration may result from a photochemical reaction which produced weak crystal binding. It is possible that a molecule within the superficial enamel might have a photochemical reaction from the excimer irradiation³⁾.

References

- 1) C. Miyazawa, et al., JAERI-M 94-017, 22(1994).
- 2) M. Kokubun, et al., J. Dent. Health, 43(1993).
- 3) C. Miyazawa, et al., Dent. in Japan, 30(1993).

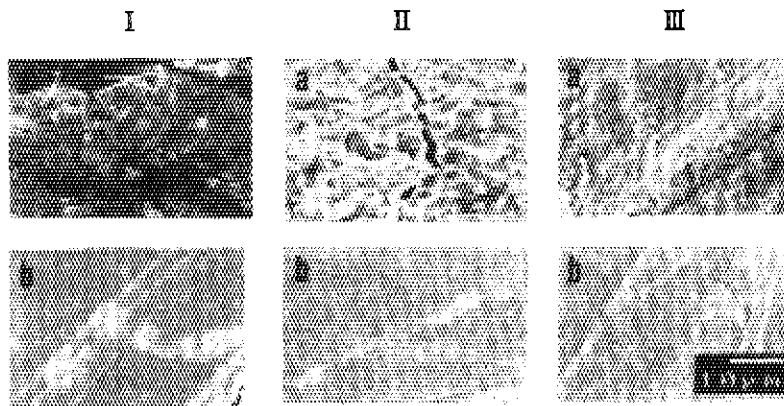


Fig. 1 The SEM findings of irradiated enamel with excimer laser beam.
 a: Before fluoridization
 b: After fluoridization

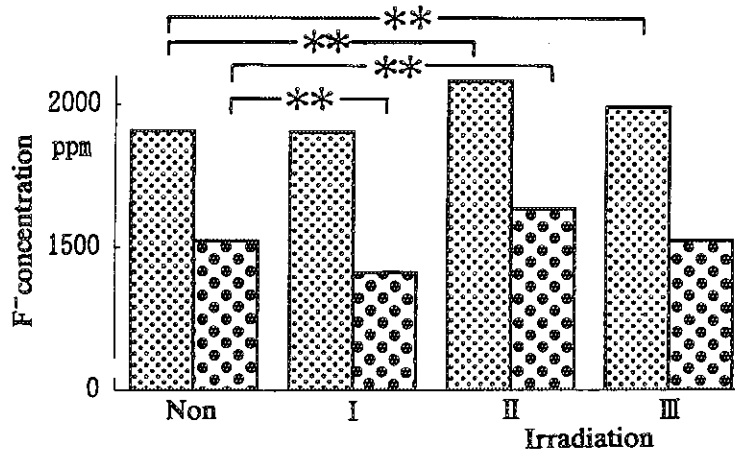


Fig. 2 The F⁻ uptake of fluoridated enamel with the excimer laser irradiation.
 [Dotted pattern] : Total F⁻ concentration
 [Cross-hatched pattern] : The F⁻ concentration in FAp
 * * : p < 0.01

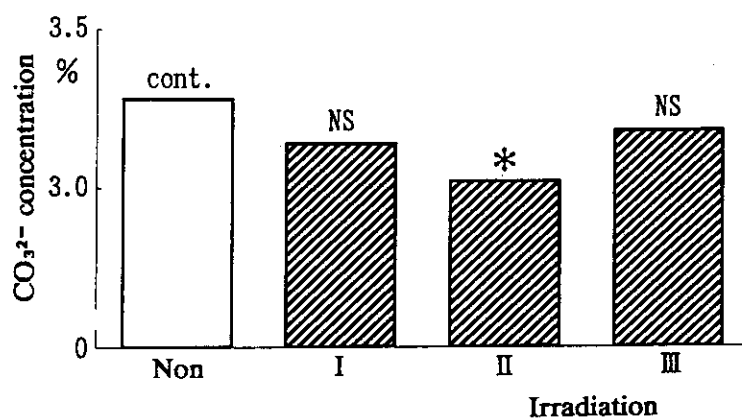


Fig. 3 The CO₃²⁻ concentration of fluoridated enamel with the excimer laser irradiation. (Fluoridated with 100ppm F⁻ for 28 days)
*: p<0.05, NS: p>0.05

9. Influence of Excimer Laser Beams on Salivary α -amylase Activity (II)¹⁾

S. Hamada*, C. Miyazawa*, M. Kokubun*, T. Shimizu*, S. Sugimoto**, Y. Shimizu,
and S. Kawanishi

Human salivary α -amylase putted into 5 different size glass cases was irradiated by excimer laser beams from a Lumonics Hyper model EX-884. Each glass case containing 1 ml of the amylase solution was irradiated with 300 shots at the fluence of 17.5 mJ/cm² pulse using a KrF excimer laser. The amount of the irradiation was divided into four parts 75 shots each. The irradiation of 75 shots was applied on the amylase solution 4 times and before each exposure the solution was stirred with an Eppendorf pipet in a glass case. The 5 types of glass cases were A (inside diameter 1 cm, area 0.79 cm²), B (i.d. 1.5 cm, area 1.77 cm²), C (i.d. 2 cm, area 3.14 cm²), D (i.d. 1.9 cm, area 2.83 cm²), E (i.d. 2.5 cm, area 4.91 cm²). The laser-irradiated amylase solution was examined for saccharifications of starch, amylase activity and electrophoresis.

Table 1 shows the results of the amylase activity in the 5 types of glass cases. The amylase activity without irradiation (control) was 730 IU/l. The amylase activity in case A was 461 IU/l resulting in a decrease of 37% in comparison with the sample of control. In case B, it was 271 IU/l, a 63% decrease. In case C, it was 146 IU/l, a 80% decrease. In case D, it was 155 IU/l, a 79% decrease. In case E, it was 108 IU/l, a 85% decrease. The amylase activity decreased with the increase in the base area of the glass case.

Figure 1 shows the saccharified zone of the laser-irradiated amylase solution after incubation for 20 hours. A halo, the zone saccharified by amylase activity, was found in all the cases. The size of the saccharified zone was 2.2 cm² for the control and 1.3, 0.9, 0.8, 0.9 and 0.7 cm² for cases A, B, C, D and E, respectively. As Table 1 shows, the size of the halo tends to decrease as the base area of the glass case become larger.

Figure 2 shows the electrophoresis of the amylase solution stained with Coomassie Brilliant Blue R250. Each lane from the right side shows the molecular weight marker of proteins (116,400, 85,200) control, and glass cases A~E. The band with a dark part in the middle of each lane is albumin. The bands of amylase and albumin in glass cases C~E were thinner than that of the control. These bands in glass cases B~E were broad and

* Department of Dentistry, Ohu University.

** Radiation Application Development Association

the molecular weight of 48,000~22,000 were found on the anode side. The size of the base area of the glass cases used in the application of laser irradiation had an influence on the α -amylase activity and saccharification of starch. These findings indicate that photochemical reaction took place only on the surface of the amylase solution.

Reference

- 1) S. Hamada et al., JAERI-M 94-017, 25(1993).

Table 1 Amylase activity

Glass case	Amylase Activity (IU/l)	Mean \pm S. D. (IU/l)
A	471.72	460.96 \pm 15.22
	450.20	
B	265.45	270.84 \pm 7.62
	276.22	
C	147.08	146.18 \pm 1.27
	145.28	
D	156.04	155.15 \pm 1.27
	154.25	
E	109.41	107.62 \pm 2.54
	105.82	

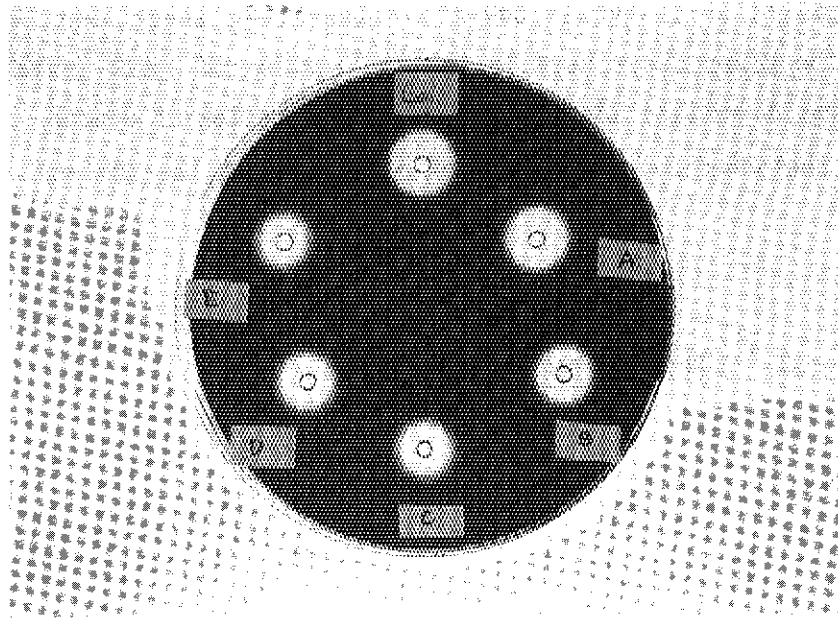


Fig. 1 Formation of halos on a starch plate after the incubation for 20 hrs with application of an excimer laser beam 300 shots.
Con. : non-irradiation,
A, B, C, D and E: glass cases A~E

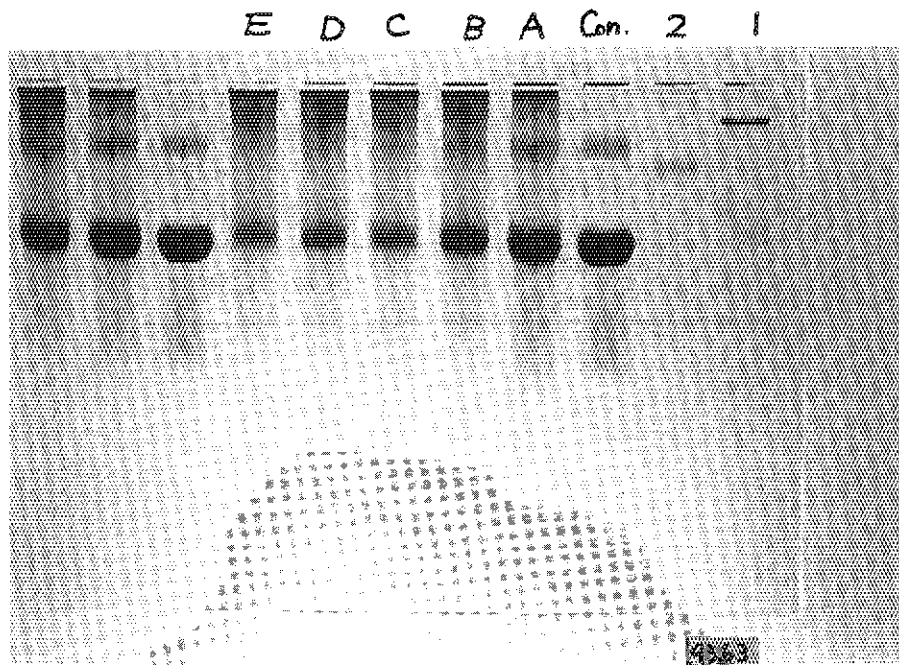


Fig. 2 SDS-PAGE of α -amylase with laser irradiation.
1: MW 116,400, 2: MW 85,200, Con. : non-irradiation,
A, B, C, D and E: glass cases A~E

10. Radiation-induced Polymerization of Spin-cased Epoxy Films

Y. Nakase, H. Doi*, and I. Fujita*

Epoxy resins are chemically stable and exhibit little contraction during the curing process and are therefore recommended as encapsulating and packing materials. Several studies were reported on ultraviolet(UV) or electron beam(EB)-initiated polymerization of epoxy oligomer resin containing polymerization-initiator in a form of cased-film of about 1 mm thickness¹⁾ or spin-cased films of several tens micrometer thickness.^{2, 3)} In this paper the polymerization induced by EB or UV irradiation of thin films, submicrometer order thickness, of epoxy resin spin-casted in air has been studied in order to know the polymerization behavior and the characteristics of polymer films obtained.

Epoxy resins used were Epikote 828 and 1001 obtained from Yuka-Shell epoxy Co. Ltd. Bis-4-[-(diphenylsulfonio)phenyl]sulfide-bis hexafluoro phosphate(BDS, Mw of 846) was obtained from General Electric Co. Ltd. and used as electron-and photo-initiator. The mixture of 828 and 1001(1:1 by weight, Mw of 640) was dissolved in tetrahydrofuran to get the oligomer solution. Solution of BDS 50wt% in propylene carbonate was added to the oligomer solution.

The chemical structure of epoxy oligomer and BDS are shown in Fig.1. The thickness of the spin-casted films on silicon wafer was determined from the absorbance at 830 cm^{-1} of key band of phenyl group using molar extinction coefficient of this band previously obtained.²⁾ Films were irradiated using a Van de Graff accelerator or a high pressure mercury arc(main wave length of 365 nm). The energies deposited in the film were estimated on the basis of CTA film dosimetry for EB, and on the basis of molar coefficients of the sample at 365 nm for UV.

For the polymerization of the epoxy oligomer, it was necessary to irradiate it with EB or UV in the presence of BDS. No polymerization reaction took place when the epoxy oligomer was heated in the presence of BDS at 130°C for 3h.

Figure 2 shows the relationship between the dose rate of EB(●) exposure rate of UV (▲) and the polymerization rates, which are measured as the decreasing rate of 916 cm^{-1} absorbance of the sample of $1.5\text{ }\mu\text{m}$ thickness. The concentration of BDS to epoxy resin is 0.5wt%, or $6\text{ }\mu\text{mole/g}$. The polymerization rate increases linearly with the increase of the dose rate or the exposure rate, which lines have the slope of 0.9. This value is close to unity and shows the characteristics of an ionic reaction mechanism.

* Osaka Electrocommunication University

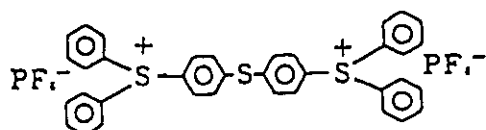
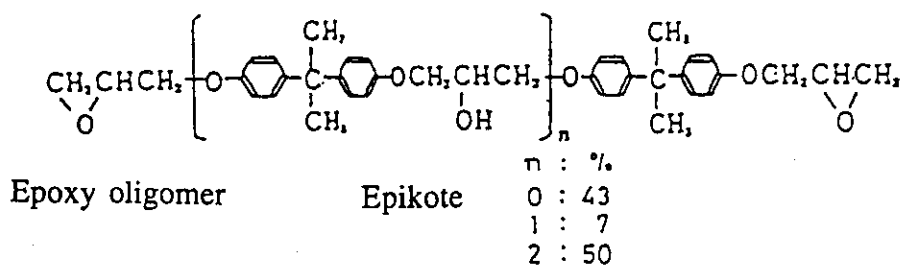
Polarized infrared spectra of the films irradiated by UV are demonstrated in Fig. 3. The solid and broken lines refer to the electric vectors parallel(0°) and perpendicular(90°) to the plane of incidence. A strong band at 830 cm^{-1} has been assigned to the CH bending vibration of benzen ring. The 830 cm^{-1} bands in the sample with the different thickness gives the strongest intensity with the polarization perpendicular to the plane. It can be concluded from these results that the benzen rings are oriented approximately parallel to the silicon wafer surface.

The electrodeposition technique is applied to study the surface characteristics of the EB-irradiated films. Copper electrodeposition, Cu-decoration, occurs in the pinholes and defects where an electrical contact between the electrode, or the film on silicon wafer, and an aqueous CuSO_4 solution exists. Figure 4 shows the Cu-decorated surfaces of two kinds of samples, $0.1\text{ }\mu\text{m}$ and $1.5\text{ }\mu\text{m}$ thickness, respectively. It is evident from Fig. 4 that few pinholes or defects can be observed in the surface of the $1.5\text{ }\mu\text{m}$ -sample, while several Cu-grain deposited on the $0.1\text{ }\mu\text{m}$ -sample to indicate the formation of pinholes.

In order to obtain the pinhole-free surface of extremely thin films, it is necessary to investigate the precise polymerization conditions including epoxy oligomer formulations.

References

- 1) T. Okada, T. Asano, M. Hatada, J. Takezaki and K. Ochi, *Kobunshi Ronbunshu* 44, 761(1987).
- 2) I. Fujita, Y. Tanaka and J. Takezaki, *J. Radiat. Phys. Chem.*, 40, 161(1992).
- 3) Y. Nakase, J. Takezaki, M. Hatada and I. Fujita, *JAERI-M* 94-017, 32(1994).



Bis -4-[-(diphenylsulfonio) phenyl] sulfide-bis hexafluoro phosphate (BDS)

Fig.1 Chemical structures of epoxy oligomer and polymerization initiator, and the composition of epoxy oligomer used.

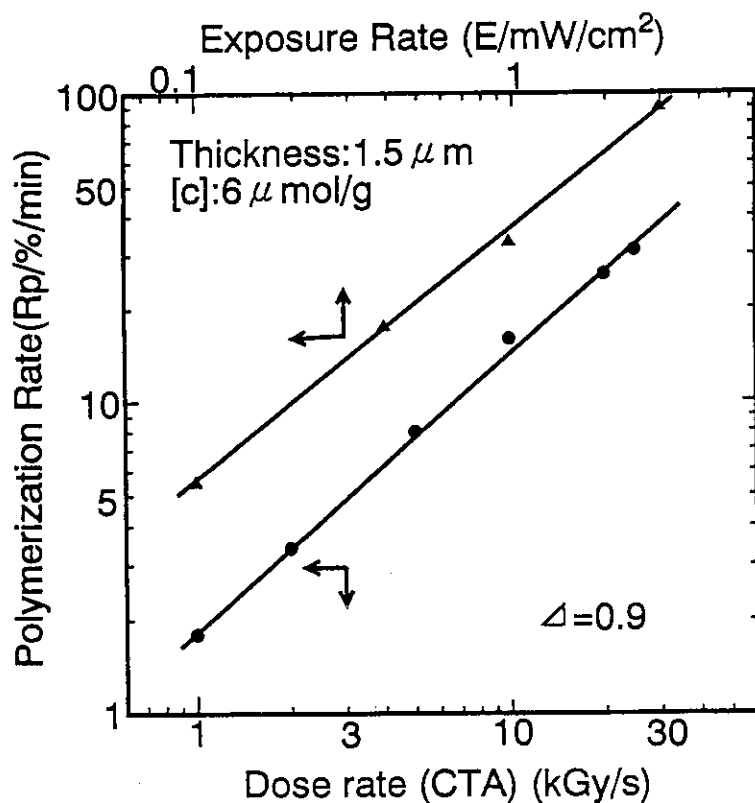


Fig.2 Relationship between polymerization rate and dose rate for electron beam, or exposure rate for ultraviolet light.

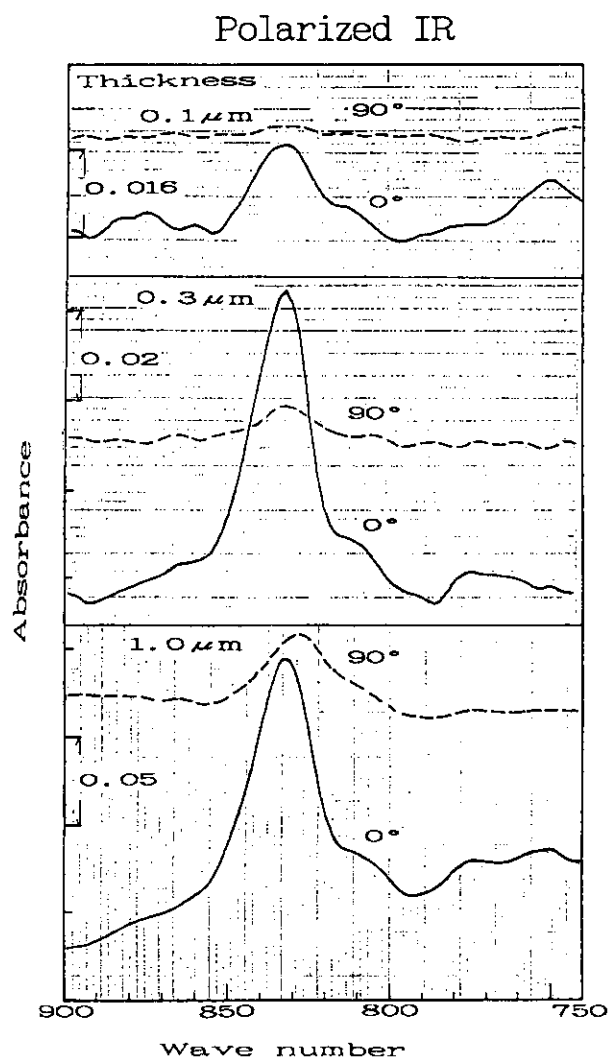
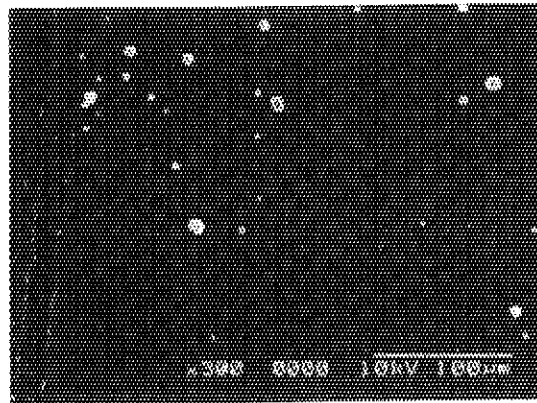


Fig. 3 Polarized refraction-absorption spectra in the CH bending region of benzen ring of epoxy oligomer film irradiated by UV. Solid and broken lines refer to the electric vectors parallel(0°) and perpendicular(90°) to the plane of incidence, respectively.

Cu-Decoration



0.1 μm

Thickness

1.5 μm

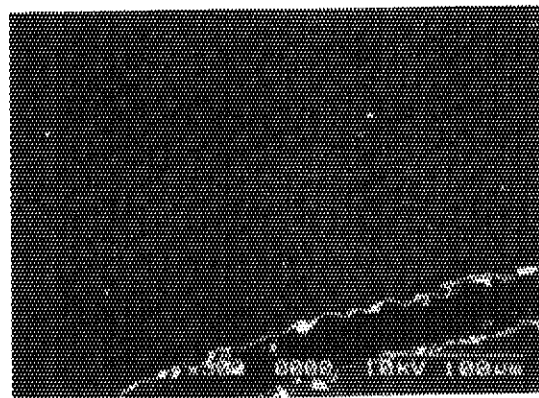


Fig. 4 Electron micrographs of spin-casted epoxy resin film irradiated by EB.
Thickness of samples is indicated in the figure.

11. Growth and Sedimentation of Fine Particles Formed in Aqueous Solutions of Palladium Sulfate by Gamma-ray Irradiation

M. Hatada and C.D. Jonah*

The mechanism of growth of palladium particles in the aqueous solution is of interest in view of the preparation of catalytic functional fine particles from aqueous solution by radiation chemical method, since the knowledge of the mechanism of formation and growth may hopefully open to the way for effective methods to prepare fine particles of desired particle size distribution. The present study has been carried out in order to know the growth of particle size during and after irradiation.

Deaerated solution of palladium sulfate (1 mM) was irradiated by gamma rays and within 3 minutes, the solutions were transferred to a cuvette for UV measurement and to a quartz tubing for dynamic light scattering in nitrogen atmosphere as described.^{1, 2)} The methods of UV measurement and DLS particle size measurement were also described.^{1, 2)}

Figure 1 shows turbidity (measured as optical density, O.D. at 700 nm) of the solution as a function of time during and after irradiation. The turbidity increased with increasing dose, indicating that the amount of metallic particles formed increased with increasing dose. However, after 15 kGy irradiation, the turbidity seems to decrease with increasing dose, suggesting that during irradiation, the particle size increased to a size large enough to sedimentate fast. The turbidity decreased just after irradiation was terminated, and the rate of turbidity decrease increased with dose. This also means that the particle size increased during irradiation.

In Fig. 2, particle size measured by DLS was plotted as a function of time during and after irradiation. It is clearly shown that the particle size increased with increasing time during and after irradiation up to 10000 sec, and it is further noticed that the plots obtained at different doses came together to rather narrow scattering range in this time range. After 10000 sec, the increase of particle size levels off for 1 - 2.5 kGy irradiation, while decrease of the particle size was observed for the solutions irradiated with larger doses, and the decrease was faster, larger the dose. These phenomena were explained by that growth of the particle size occurred after irradiation, but more closely packed particles were formed during irradiation, and therefore the sedimentation rate is larger in the solution irradiated with larger doses.

* JAERI Foreign Researcher (ANL)

To draw a rough picture of the particles, a simple calculation was made in the following. Assuming that the floating particles in an optical path of a cuvette resulted the observed turbidity without overlapping of the particle in the optical path, eq. (1) is obtained.

$$I/I_0 = 10^{-OD700} = (1 - n \ell \pi r^2) = 1 - n \pi r^2 \quad (1)$$

where I_0 and I are the intensities of light before and after passing through the solution, respectively; OD700 is optical density at 700 nm, ℓ is optical path length, r is average diameter of particle and n is number of particles in 1 ml solution. Since visual examination of the solution immediately after irradiation indicated no precipitation of solid at the bottom of the irradiation vessel, it is further assumed that mass of all ions consumed in the solution is equal to the mass of the particles. This leads to the following equation:

$$\begin{aligned} \{\Delta OD389 / \epsilon 389\} \times \{A/1000\} &= 4/3 \cdot \pi r^3 n d \quad (2) \\ -m[Pd^{2+}] &= \Delta OD389 / \epsilon 389 = Pd_m \quad [\text{mol/l}] \end{aligned}$$

where A is the atomic number of palladium (=106.42), d is average density of the particles, $\Delta OD389$ is the decrease of optical density at 389 nm by irradiation, and $\epsilon 389$ is molar extinction coefficient of $[Pd(H_2O)]^{2+}$ at 389 nm. Combination of these equations resulted in the following equation:

$$\begin{aligned} d &= \frac{\{\Delta OD389 / \epsilon 389\} \times \{106.42/1000\}}{4/3 \cdot \pi r (1 - 10^{-OD700})} \\ n &= (1 - 10^{-OD700}) / \pi r^2 \end{aligned}$$

Several examples of calculations using sets of $\Delta OD389$, OD700, and r taken at 300, 10000 and 30000 sec after irradiation from Figs. 1 and 2 are shown in Table 1. The d_w in the table is the density of the particle calculated from d value on the assumption that cavities in a particle are filled with water molecules so that the fill factor, FF may be 0.74 for f.c.c. value.

The results of calculation seem to give us rough image of shape and growth of particles in the solution. Take the result obtained for 1 kGy irradiation for example, the average density of particle including water (3.61 g/cm^3) decreases with time, the average number of Pd atoms ($3 \times 10^7/\text{particle}$) in a particle increased, and the average number of particles in the solution ($9.5 \times 10^8/\text{cm}^3$) decreases with time, showing gradual growth of particles by mutual get-together coagulation of particles forming bulky particles. Sedimentation rate (SV) calculated on the basis of Stokes' law seems to

be reasonable to explain sedimentation curve obtained on UV spectrophotometer. However, the calculations for the particles obtained by higher doses (>10 kGy) and longer elapsed time gave unreasonable values indicated by parenthesis in the table. This is because at these conditions, precipitation was observed at the bottom of the vessel and the assumption that all ions consumed is floating in the solution as non-transparent particles is no longer valid.

References

- 1) M. Hatada, JAERI-M 93-232 (1993).
- 2) C. D. Jonah and M. Hatada, JAERI-M 93-248 (1994).

Table 1 Density, diameter, number of Pd atoms in a particle and other related values concerning Pd particle in solution

D	t	SV	dw	NP	NPd	-[Pd ²⁺]	FF	DM
1	300	4.59E-06	3.61	0.949E+09	0.294E+08	0.463E-04	0.106	180
	10000	3.46E-05	2.51	0.648E+08	0.431E+09	0.463E-04	0.033	650
	3000	7.86E-05	2.45	0.202E+08	0.138E+10	0.463E-04	0.029	1000
2.5	300	7.84E-06	3.98	0.101E+10	0.663E+08	0.111E-03	0.131	220
	10000	4.64E-05	2.74	0.842E+08	0.795E+09	0.111E-03	0.049	700
	30000	1.14E-04	2.90	0.205E+08	0.326E+10	0.111E-03	0.059	1050
5	300	1.74E-05	5.09	0.732E+09	0.213E+09	0.259E-03	0.204	280
	10000	8.50E-05	3.78	0.661E+08	0.236E+10	0.259E-03	0.118	750
	30000	2.49E-04	5.58	0.139E+08	0.113E+11	0.259E-03	0.237	1000
10	300	4.20E-05	5.83	0.397E+09	0.772E+09	0.509E-03	0.254	400
	10000	1.60E-04	5.08	0.515E+08	0.596E+10	0.509E-03	0.204	850
	30000	(8.38E-04)	(14.99)	(0.646E+07)	(0.475E+11)	0.509E-03	(0.862)	1050
15	300	7.37E-05	6.42	0.266E+09	0.174E+10	0.769E-03	0.293	500
	10000	2.97E-04	6.46	0.330E+08	0.140E+11	0.769E-03	0.295	1000
	30000	(7.50E-04)	(33.66)	(0.169E+08)	(0.274E+11)	0.769E-03	(2.101)	650
20	300	1.59E-04	6.21	0.108E+09	0.560E+10	0.100E-02	0.279	750
	10000	(5.06E-04)	(12.50)	(0.249E+08)	(0.241E+11)	0.100E-02	(0.696)	900
	30000	(8.51E-04)	(112.41)	(0.328E+08)	(0.184E+11)	0.100E-02	(7.329)	375

D:dose (kGy); t:time (sec); SV:sedimentation velocity; dw:density of particles;
 NP:number of particles per ml solution; NPd:number of Pd atoms in a particle;
 FF:fill factor; DM:diameter (nm).

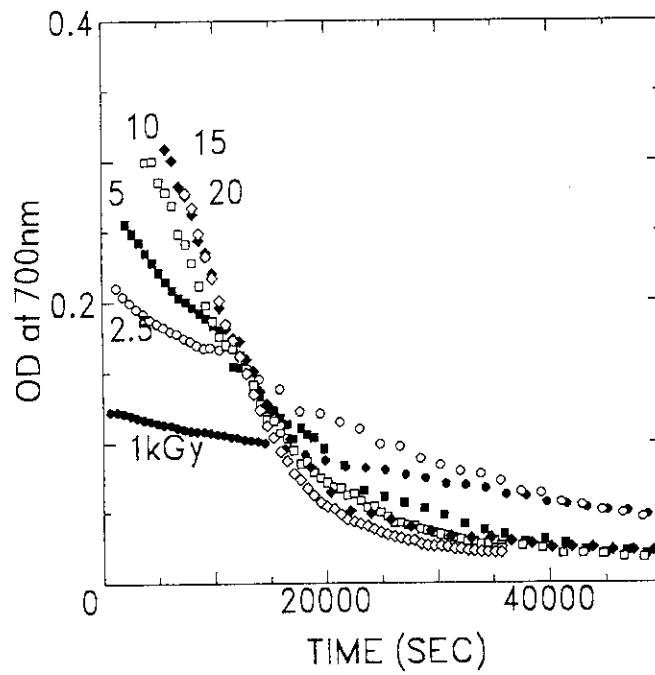


Fig.1 O.D. at 700 nm as a function of time during and after irradiation; numerals in the figure denote dose in kGy.

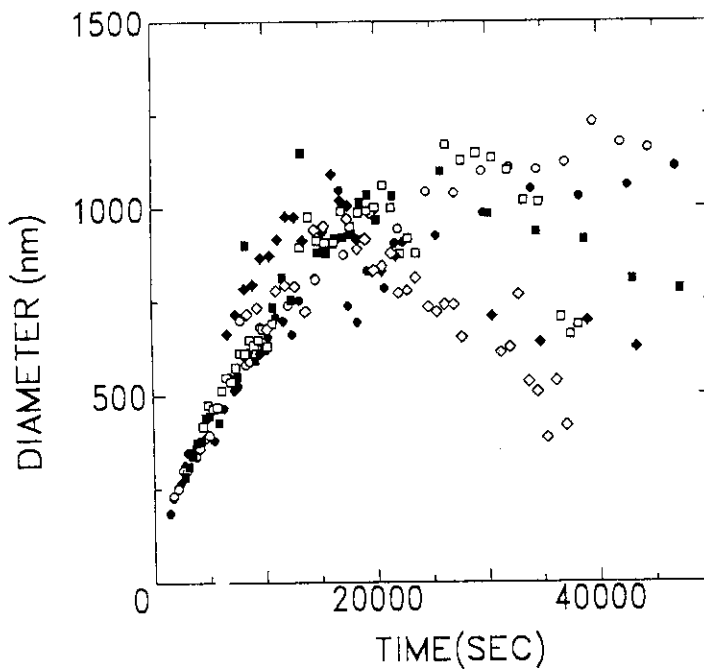


Fig.2 Diameter of particles as measured by DLS method;
 ● 1; ○ 2.5; ■ 5; □ 10; ◆ 15; ◇ 20 kGy.

12. Formation of Palladium Clusters and Particles from Aqueous Solution of Sodium Chloro-palladate by Gamma-ray Irradiation

M. Hatada, I. Fujita* and K. Korekawa*

In the previous papers,^{1, 2)} we reported that palladium particles were formed in deaerated palladium sulfate aqueous solution by gamma ray irradiation and that the particles grow during irradiation and after irradiation as well. The estimated density of the particle formed after 1 kGy irradiation is 3 and average diameter of the particles is about 200 nm, indicating that the particles are loosely combined palladium atoms or clusters with water molecules in-between. However, we could not observe clusters which are reported to have absorption maximum at about 308 or 386 nm experimentally³⁾ in the presence of organic stabilizer and at ca. 220 nm theoretically.⁴⁾

Since it is reported that the presence of sulfate ion results rapid disappearance of palladium cluster,³⁾ we have carried out gamma ray irradiation on aqueous solution of sodium chloropalladate instead of palladium sulfate in order to know whether it is possible to observe palladium clusters, and irradiation effects have been studied by UV spectrophotometry and dynamic light scattering technique (DLS). Reactivities of different ligand configurations of the palladate complex ion are also a subject of the present study.

The experimental methods were the same as those described in the previous reports.^{1, 2)} Aqueous solutions of pH=1.95 and 0.65 containing 0.3mM sodium chloropalladate were prepared by dissolving solid sodium chloropalladate in corresponding hydrochloric acid and hydroperchloric acid. The solution was deaerated with bubbling argon gas before the gamma ray irradiation. The doses were from 2.75 to 16 kGy.

In Fig.1, the spectra of the un-irradiated solutions of pH=1.95 by HCl (a), of pH=0.65 by HCl (b), and pH=1.95 by HClO₄ (c), and pH=0.65 by HClO₄ (d) are shown, respectively. By comparison of the spectra with those reported⁵⁾, the spectra were assigned to [PdCl_n(H₂O)_{4-n}]²⁻ⁿ of different n's; (a) n=2, 3: [3][>][2], (b) n=4, and (c) and (d) n=2, 3: [2][≅][3], respectively.

The spectra obtained immediately after the irradiations of different doses for the solution (a) are shown in Fig.2, where it is noted that (i) absorptions at 208 and 238 nm due to palladate ion decreased with increasing dose and disappeared above 8

* Osaka Electrocommunication University

kGy, and (ii) broad absorption toward longer wave length to 700 nm (which is not clear in the figure) increased with increasing dose, but above 8 kGy, it decreased with dose. The results show that the palladate ion was consumed by irradiation and non-transparent particles were formed by the irradiation and that the broad absorption is possibly due to palladium cluster.

In Fig. 3, absorption at 700 nm was plotted as a function of time after irradiation at different doses. The absorption increased with time after irradiation and then decreased with time, except the curve obtained at 11 kGy irradiation which decreased monotonously with time. The increase of the absorption indicates that precursors, possibly, small size clusters of several palladium atoms, which do not absorb light at 700 nm, combined together to form particles which absorb light at 700 nm. The decrease of absorption at 700 nm indicates that the particles go to sedimentation by further coagulation.

In Fig. 4, absorption at 238 nm was plotted as a function of time obtained for the same solutions of different doses. The absorption at time 0 decreased with irradiation dose indicating that the palladate ion decreased with dose as mentioned before. It is noted that the absorption increased with increasing time. This means that some product formed from the palladate, possibly cluster, reacted backwards with chloride ion to form palladate. The rate of backward reaction was highest for the solution irradiated by 5.5 kGy. This may qualitatively be explained by that at dose below 5 kGy, the rate is small since the amount of the cluster is small, and at dose above 5 kGy, the rate also becomes small since the clusters had been combined to form large particles which no longer reacted to form palladate.

DLS measurement revealed that average diameter of the particles after irradiation is 50 nm which is smaller than those observed for palladium sulfate solution.

For solutions (b), (c), and (d), different results from those obtained for solution (a), suggesting that the radiation effects depend on configuration of ligands of the palladate ion. The detailed studies on this point is in progress.

References

- 1) M. Hatada, JAERI-M 93-232 (1993).
- 2) C. D. Jonah and M. Hatada, JAERI-M 93-248 (1994).
- 3) M. Michaelis and A. Henglein, J. Phys. Chem., 96, 4719 (1992).
- 4) J. A. Creighton and D. G. Eadon, J. Chem. Soc. Faraday Trans., 87, 3881 (1991).
- 5) L. I. Elding, Inorg. Chimica Acta, 6:4, 648 (1972).

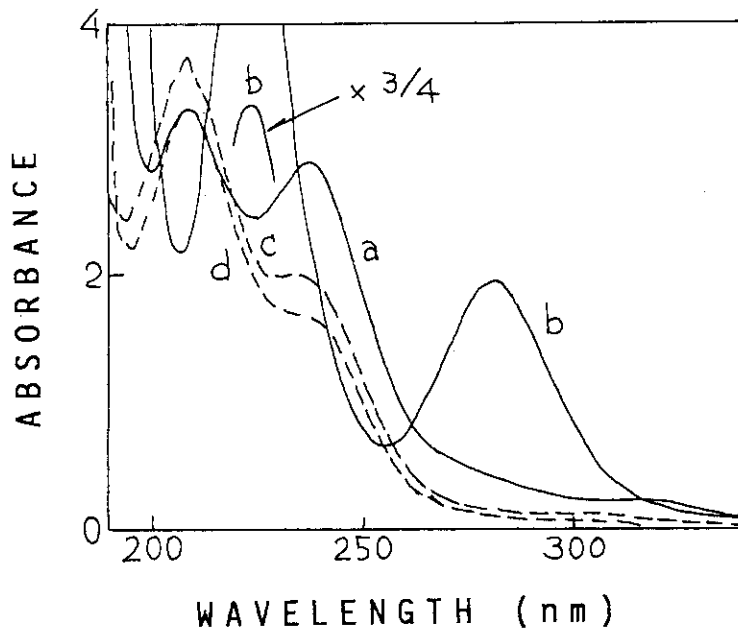


Fig.1 Electronic spectra of un-irradiated sodium chloropalladate solutions; pH=1.95 by HCl (a), of pH=0.65 by HCl (b), and pH=1.95 by CH_1O_4 (c), and pH=0.65 by CH_1O_4 (d).

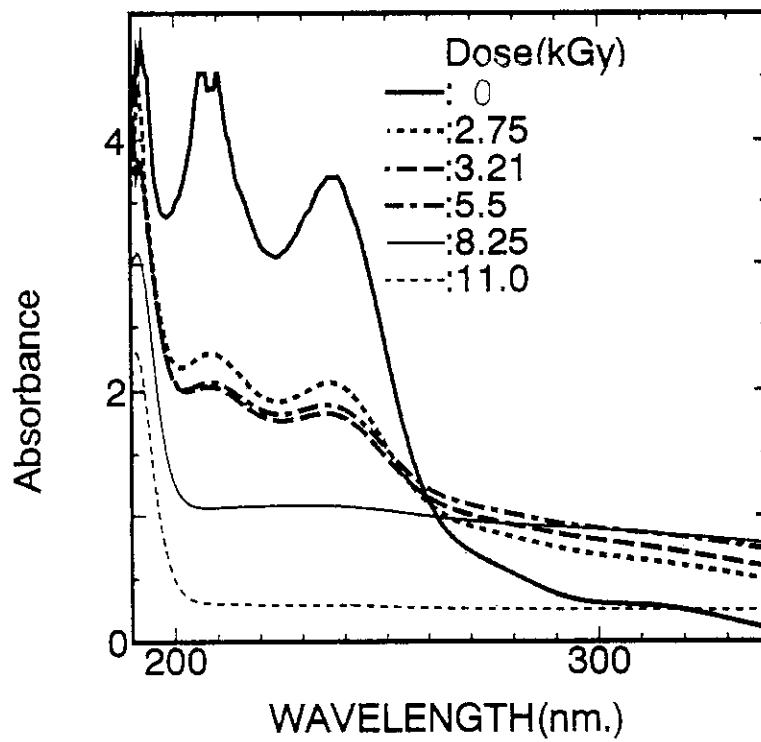


Fig.2 Electronic spectra of un-irradiated and irradiated sodium chloropalladate solutions; pH=1.95 by HCl.

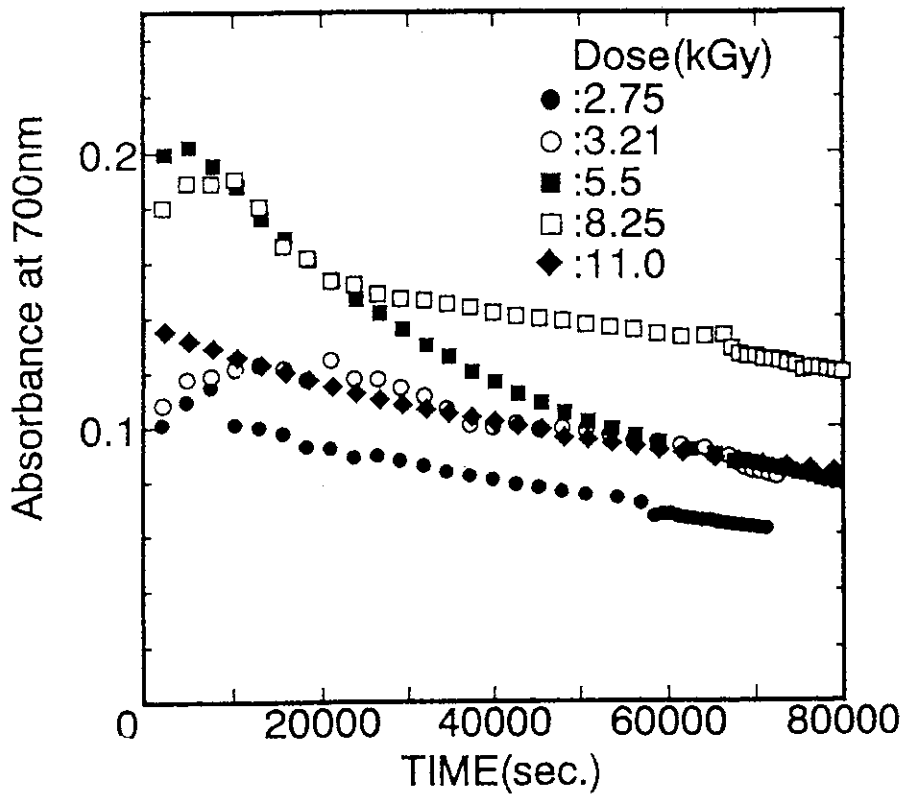


Fig.3 Absorbance at 700nm as a function of time after irradiation.

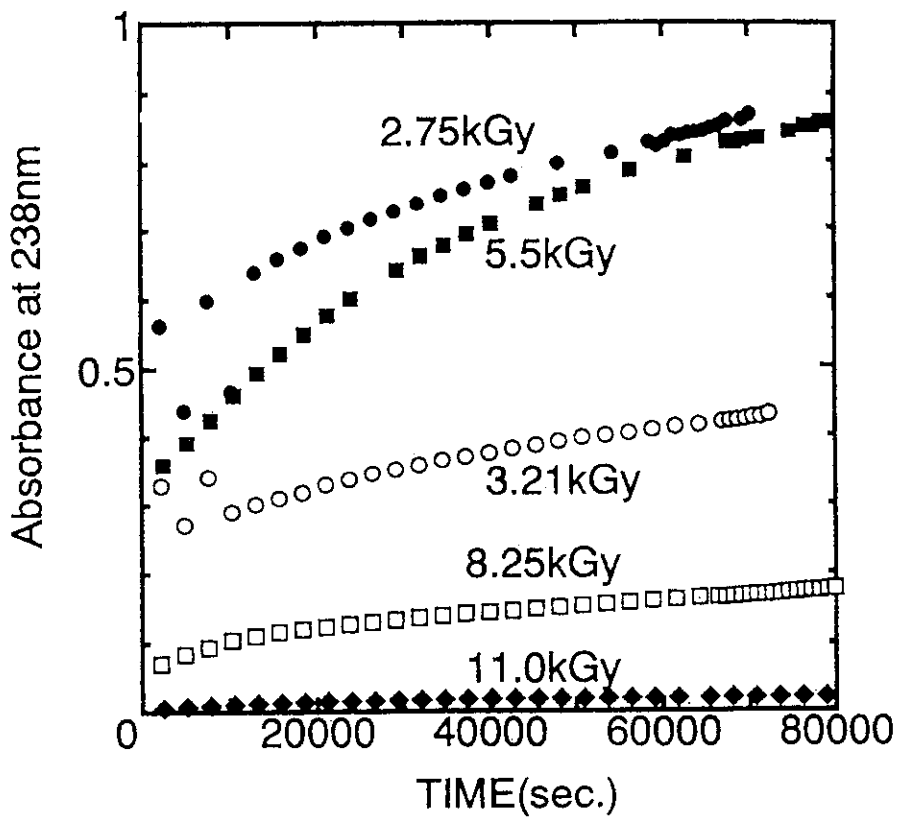


Fig.4 Absorbance at 238nm as a function of time after irradiation.

13. Photo-emission from Excited CO_2^+ Ion by High Energy Electron Irradiation of Neon-carbon Dioxide Gas Mixture

K. Nakato, M. Uehara*, I. Fujita*, and T. Kijima

The knowledge of energy transfer from rare gas to simple molecules is important for rare gas-sensitized radiolyses of the simple molecules. As a series of studies¹⁻⁵⁾ to obtain data on energy transfer between rare gases and the simple molecules, studies on photo emission from gas mixtures of helium and carbon monoxide,²⁾ and helium or argon carbon dioxide^{4, 5)} excited by electron irradiation were carried out. This year, in comparison with these mixtures, we have made some measurements of emission spectra from excited states of carbon dioxide(CO_2^{+*} (A, B)) formed by electron irradiation of gas mixture of neon and carbon dioxide in order to study energy transfer scheme involving these species, which explains experimental data of emission intensities obtained under different gas compositions and gas pressures.

Experimental set up and experimental procedures used in the present study are described elsewhere.^{1, 2)} Carbon dioxide gas and neon gas were obtained from Takachiho Chemicals Co. and Sumitomo Seika Chemicals Co., respectively. Electron irradiation was carried out with 0.6 MeV electrons from a Van de Graaff accelerator.

Figure 1(a) shows emission spectra obtained by electron irradiation of carbon dioxide at pressure of 300 torr. Two emission bands were observed, one due to the $\text{A}\Pi-\text{X}\Pi$ (A-X) transition, and the other $\text{B}\Sigma-\text{X}\Pi$ (B-X) transition from CO_2^{+*} . Figure 1(b) shows emission spectra from mixture of carbon dioxide and neon gas. The (A-X) band systems are disturbed by emission from impurity such as N_2 , OH, etc. in gases.

Figure 2 shows emission intensities of (B-X) band systems plotted as a function of partial pressure of carbon dioxide, the pressure of argon being taken as a parameter. Table 1 shows a possible scheme tentatively assumed from those established for other mixture of rare gas and the simple gases(CO-He), ($\text{CO}_2\text{-He}$) in the earlier studies.^{2, 4)} With increasing the partial pressure of carbon dioxide, the emission intensities of (B-X) band increased and the approached to a constant value. This indicates that more CO_2^{+*} were formed by direct excitation of carbon dioxide (reaction (1)) with increasing carbon dioxide pressure, and more quenching of CO_2^{+*} due to collision with carbon dioxide molecules (reaction (2)) occurred when the carbon dioxide pressure increased further. Increase of the emission is observed down to low pressure of carbon dioxide below 1 Torr. This may be explained by that many CO_2^{+*} are formed by Penning ionization due to collision with excited neon atom (reaction (7)).

* Osaka Electrocommunication University

At a pressure of carbon dioxide of above 1 Torr, the emission decreased with increasing neon pressure, indicating that quenching of CO_2^{+*} due to collision with neon (reaction (4)) took place.

These results may be explained by the reaction mechanism (Table 1), which further leads to the following equation under a steady state approximation on intermediates:

$$[\text{CO}_2^{+*}] = \frac{[\text{CO}_2] / (k_Q [\text{CO}_2] + k_R + k_{QN} [\text{Ne}])}{\{B_{C_2} + k_{C_2} B_N [\text{Ne}] / (k_{D_2} [\text{Ne}] + k_{C_2} [\text{CO}_2])\}} \quad (1)$$

where B_{C_2} , k_Q , k_{C_2} , etc. are the rate constants. The species in brackets represent the concentrations of the corresponding species. The first term in equation (1) indicates the amount of CO_2^{+*} formed by direct excitation due to collision with electron, and the steady state concentration of CO_2^{+*} which increases monotonously to a constant value with increasing carbon dioxide concentration. The second term indicates the amounts of CO_2^{+*} formed by Penning ionization due to collision with excited neon atoms, and the steady state concentration of CO_2^{+*} becomes a maximum at carbon dioxide concentration given by equation (2):

$$[\text{CO}_2] = \{k_R k_{D_2} [\text{Ne}] / (k_Q k_{C_2})\}^{1/2} \quad (2)$$

For infinitely large carbon dioxide concentration in equation (1), concentration of carbon dioxide becomes constant value as given by equation (3):

$$\lim_{[\text{CO}_2] \rightarrow \infty} [\text{CO}_2^{+*}] = B_{C_2} / k_Q \quad (3)$$

This agrees well with the experimental result that the emission intensities from excited species approach a constant value with increasing carbon dioxide pressure. The second term of equation (1) may account for the increase observed for emission intensities at pressure of carbon dioxide in Fig. 2.

Although the analysis on the (B-X) band was successful mentioned above, the (A-X) band systems could not be carried out, because this band systems were disturbed by other emission spectra as shown in Fig. 1(b).

It was found that the reaction schemes which explain the intensities of photo-emissions under different reaction conditions of Ne- CO_2 system are the same as those obtained for the He- CO_2 and Ar- CO_2 systems in the previous studies regardless of different masses of the rare gases included in the systems.

References

- 1) K. Matsuda, et al., Appl. Radiat. Isot., 41, 757(1990).
- 2) K. Matsuda, et al., Appl. Radiat. Isot., 42, 1223(1991).
- 3) I. Fujita, et al., Appl. Radiat. Isot., 43, 641(1992).
- 4) K. Nakato, et al., unpublished data.
- 5) K. Nakato, et al., unpublished data.

Table 1 Reaction scheme

Reactant	Product	Rate Constant	Type of reaction	
$\text{CO}_2 + e$	\longrightarrow CO_2^{*+}	$B_{e,2}$	Excitation	(1)
$\text{CO}_2^{*+} + \text{CO}_2$	\longrightarrow $\text{CO}_2^{*+} + \text{CO}_2$	k_Q	Quenchig	(2)
CO_2^{*+}	\longrightarrow $\text{CO}_2^{*+} + h\nu$	k_R	Radiation	(3)
$\text{CO}_2^{*+} + \text{Ne}$	\longrightarrow $\text{CO}_2^{*+} + \text{Ne}$	k_{QN}	Quenchig	(4)
$\text{Ne} + e$	\longrightarrow Ne^*	B_N	Excitation	(5)
$\text{Ne}^* + \text{Ne}$	\longrightarrow $\text{Ne} + \text{Ne}$	k_{D2}	Deactivation	(6)
$\text{Ne}^* + \text{CO}_2$	\longrightarrow $\text{Ne} + \text{CO}_2^{*+}$	k_{C2}	Excitation Transfer	(7)

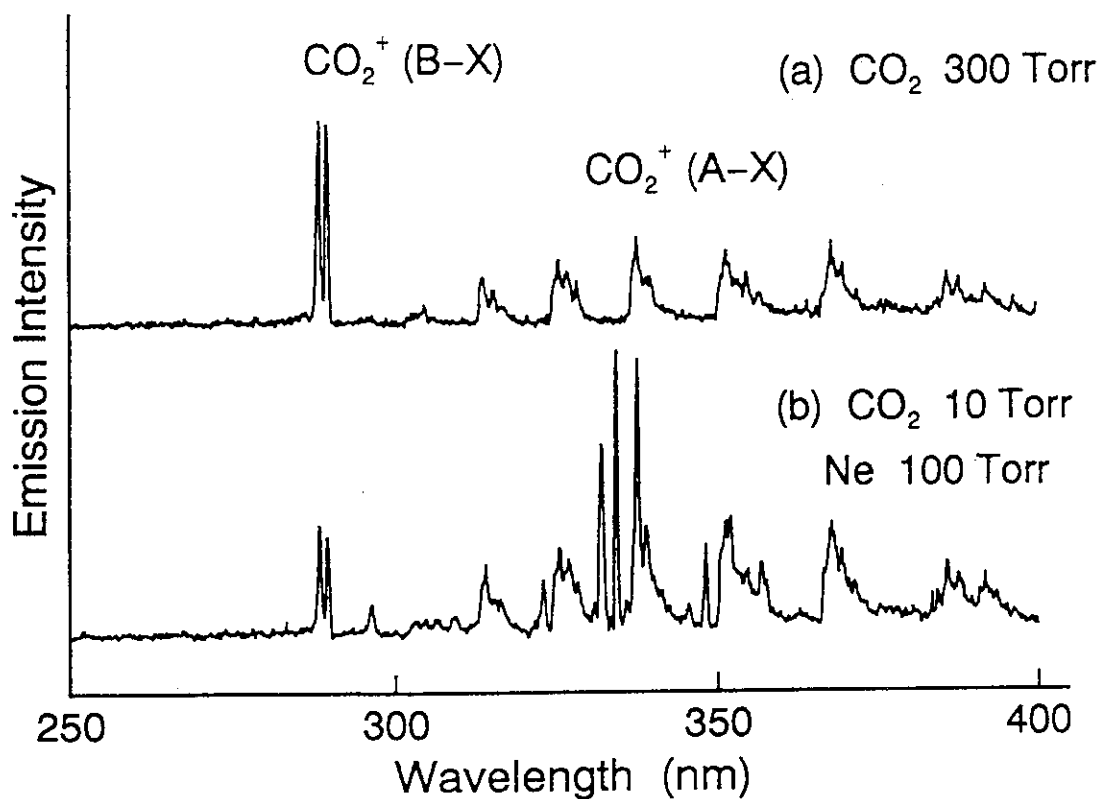


Fig.1 Emission spectra of carbon dioxide.

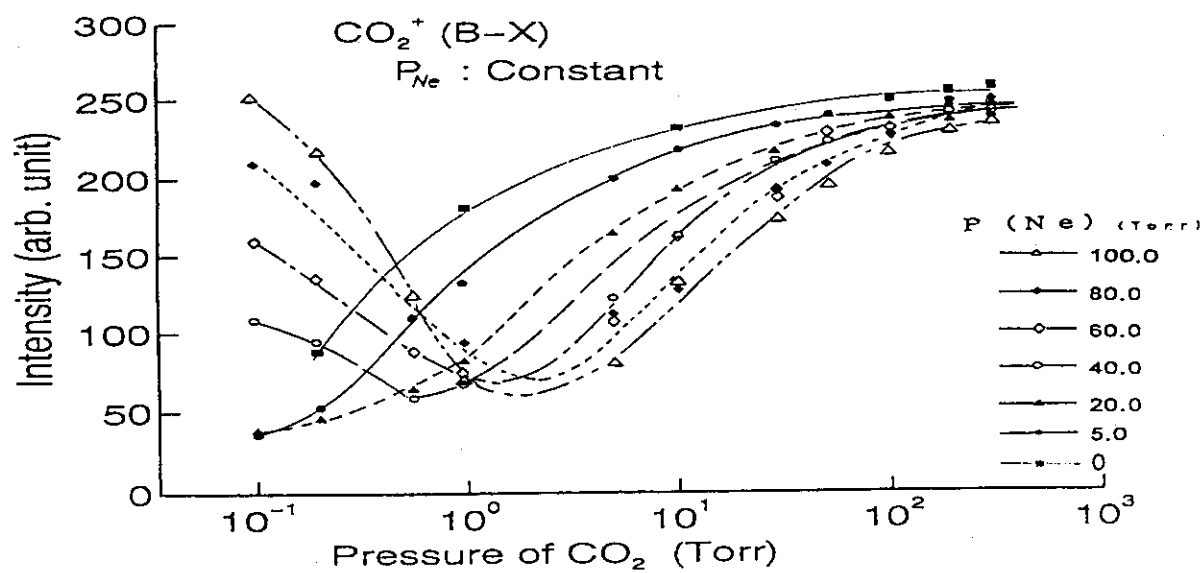


Fig.2 Emission intensities of (B-X) band.

14. Depth-dose Distributions in a Thin-layer Absorber Irradiated by 300 keV Electrons

T. Kijima, K. Nakato and Y. Nakase

In the industrial utilization of electron beam irradiation, depth-dose distributions of irradiated material is important to both the planning and routine operation to keep sufficient quality control. In radiation curing of thin-layers on a plate and of laminated polymer such as coatings by low-energy electron beams, estimations of the depth-dose distribution depends on the thickness of the layer and the atomic number of backing material. In these dose estimation, thin layer dosimeter such as cellulose triacetate film(CTA) is used.

Monte Carlo calculations of low-energy electron-beam dose distributions in various absorbing media have shown general agreement with thin-film dose measurements, as long as simple multi-layer geometries are used.¹⁾ Such calculations can be useful for estimating transmission and reflection of electrons, electron fluence spectra, their angular distributions, their back-scattering and depth-dose distributions. We have investigated the factors influencing depth-dose distributions of a thin CTA film by Monte Carlo radiation transport calculations, especially the difference between the influences of dynamic and static irradiation, and also the dose estimation at the film surface.

The validity of our calculation code was at first considered. Figure 1 shows the calculated and experimental results of depth-dose distributions of several electron energies in typical metal(Al) and organic material(polystyrene) absorbers of semi-infinite thickness(mono-layer). In Fig. 1, plots of 314 and 521 keV of Al(open circles) and 400 keV of polystyrene(filled circles) are quoted from experimental data^{2, 3)} and plots of 200 keV of Al(open circles) are the calculated values by ITS.⁴⁾ Solid and broken curves are from our calculations which show good agreement with the plots indicating good accuracy for the low-energy region in the range 200-521 keV.

Figure 2 shows experimental results compared with the calculated results of depth-dose distributions in a multi-layer absorber (Ti-Air-CTA) shown in our previous paper.⁵⁾ Here a simple multi-layer geometry of Ti(0.03 mm), air gap(10 cm) and CTA of semi-infinite thickness for 300-keV electron is considered. Calculated results show good agreement both in the cases of dynamic and static irradiation except in the region at depths $< 0.01 \text{ g} \cdot \text{cm}^{-2}$ (ca. 0.04 on the abscissa) from the entrance surface of CTA.

The difference between the peaks of depth-dose distributions in CTA irradiated by dynamic and static irradiation is investigated. Electron fluence spectra for 300-keV are

calculated at the beam center (0 cm) and at 5, 10 and 20 cm from the beam center across the beam scanning direction in the case of static irradiation as shown in Fig. 3. In Fig. 3, the solid curves of the electron spectra show the spectra including the effect of backing material (CTA), while the broken curves show the spectra of direct incident electrons without backscattering. The 300-keV electron beams, after passing through the Ti window and air gap, give peak values (the most probable electron energy) of 248 keV at the beam-scan center, and 240, 231 and 202 keV at 5, 10, 20 cm lateral distance. These decreases of the most probable electron energy and the broadening of electron spectra are likely due to that lower energy electrons are scattered more in the increased air gap. The effect of backscattering can be observed in the region of 20-210 keV electron energies.

Figure 4 shows, for the cases of static irradiation, the calculated depth-dose distributions in CTA of semi-infinite thickness at the beam-scan center and at 5, 10 and 20 cm across the beam scanning direction. The solid curves show depth-dose distributions of penetrating diffusely incident electrons. The broken curves show depth-dose distributions by assuming all the incident electrons come vertically (perpendicularly) to the surface in the final step of trajectories. For the latter calculation of perpendicularly incidence of electrons at sample surface, their energy distributions and number of electrons were assumed to be the same as the diffuse incidence case except for the incident angles. The depths of the maximum dose (the depth of the depth-dose peak), therefore, shift more and more toward the entrance surface for both diffuse incidence and hypothetical perpendicular incidence as the lateral distance from the beam-scan center increases. In the case of the diffuse incidence, the position of the maximum dose shifts toward the entrance surface at a greater rate than in the case of the hypothetical perpendicular incidence. The factor which causes the forward shift of the depth-dose peak in the case of dynamic irradiation compared with static irradiation is suggested to be mainly the greater angle of incidence of electrons at the surface of the absorber.

Figure 5 shows the calculated and the experimental data of depth-dose distributions in three layers of thin CTA film (0.114 mm thickness) on different backing materials (CTA, Al, Fe, Sn and Pb) for the charge fluence rate $0.047 \mu\text{C} \cdot \text{cm}^{-2} \cdot \text{s}^{-1}$. The calculated and experimental results show good agreement in the case of all backing materials.

By the theoretical analysis by a Monte Carlo simulation method, the major factor for explaining the peak shift at the dynamic irradiation can be the increase of incident angle of the incident electrons rather than a decrease in the incident electron energy. Monte Carlo calculations of 300-keV electron beam dose distribution have shown good

agreement with experimental depth-dose measurements at low dose rate.

References

- 1) W.L. McLaughlin, H.M. Kahn, M. Farahani, M.L. Walker, J.M. Puhl, M. Seltzer, C.G. Soares and C.E. Dick., *Beta-Gamma* 4(2+3), 20, 1991.
- 2) G.L. Lockwood, G.H. Roggles, G.H. Miller and J.A. Halbleib, Sandia Labs. Rept., SAND79-0414, 1980, Albuquerque, NM.
- 3) W.L. McLaughlin and E.K. Hussmann, Proc. of Symp., Munich, 1969, IAEA STI/PUB/236, International Atomic Energy Agency, Vienna, pp. 579.
- 4) P. Andreo, R. Ito and T. Tabata, Res. Inst. Adv. Sci. Tech. Univ. Osaka Prefect. Tech. Rep. No.1, 1992, Osaka, Japan.
- 5) T. Kijima and Y. Nakase, *Appl. Radiat. Isot.* 44, 693(1993).

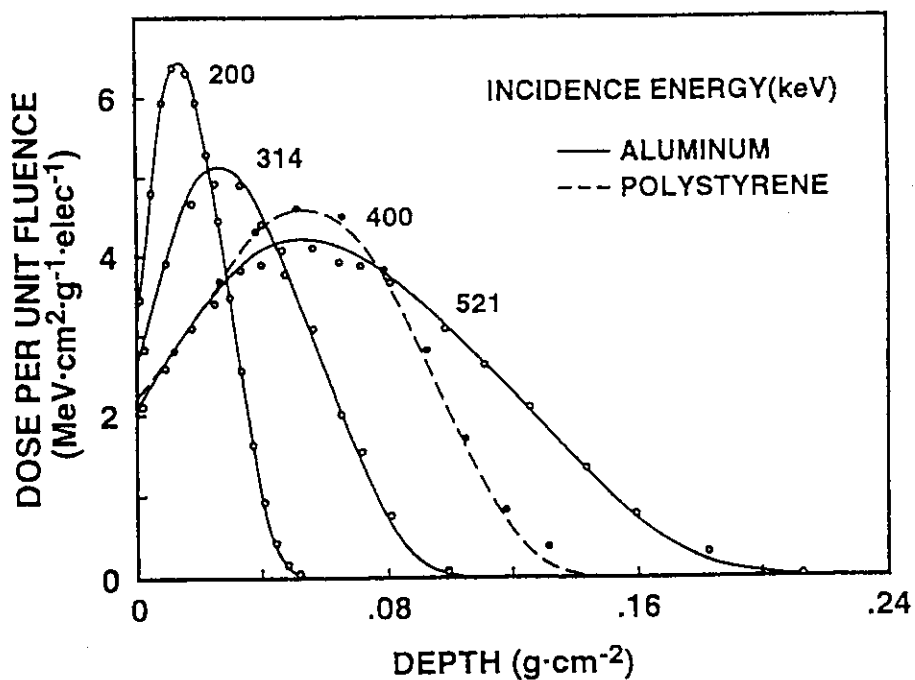


Fig.1 Comparison of experimental data(points) and calculated(solid and broken lines) depth-dose in semi-infinite aluminum(\circ) and polystyrene(\bullet) mono-layers for electrons with various energies.

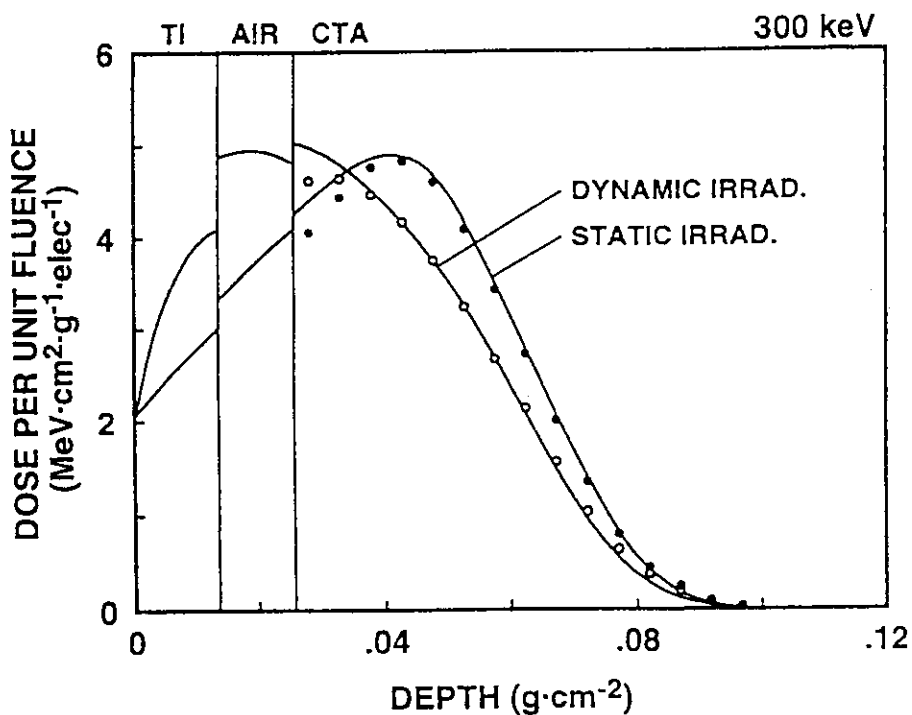


Fig.2 Comparison of experimental data(points) and calculated(solid lines) depth-dose distributions for 300-keV electrons in totally absorbing CTA film stacks for electron beam traveling the 0.003-cm Ti window and 10-cm air gap, with dynamic or static scanning irradiation.

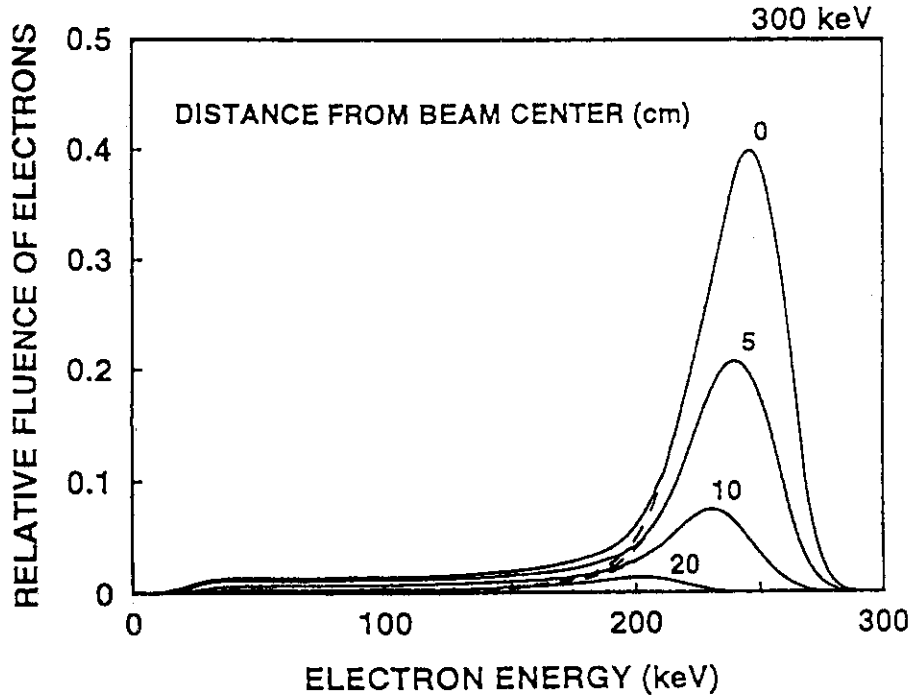


Fig. 3 Calculated electron fluence spectra at the semi-infinite CTA surface for 300-keV electrons after passing through the 0.003-cm Ti window and 10-cm air gap at several lateral distances from the beam center, for static irradiation.

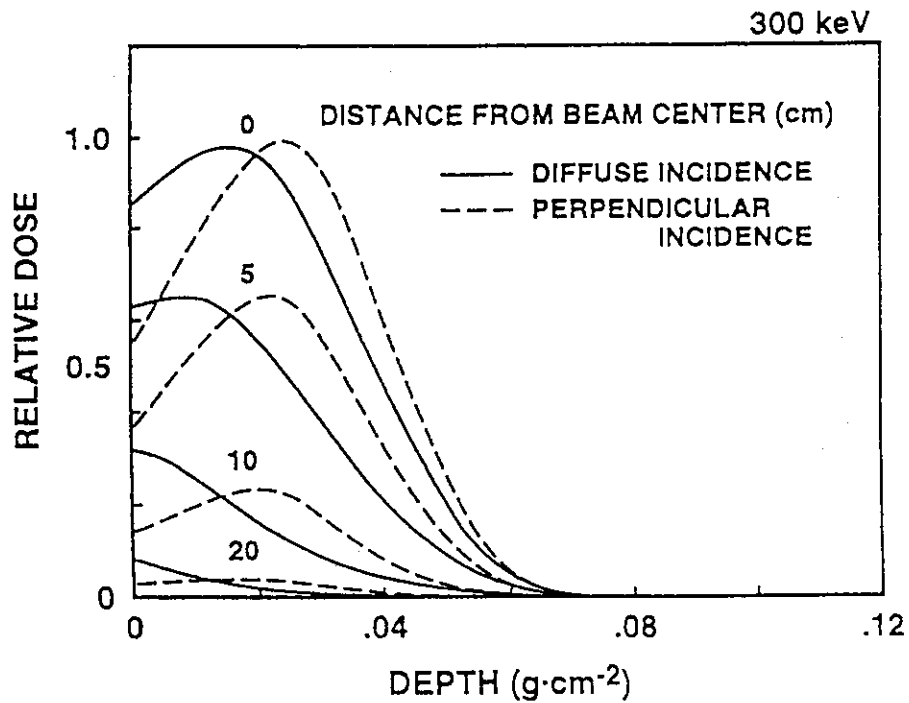


Fig. 4 Comparison of depth-dose distributions of perpendicular(hypothetical) and diffuse(real) incidence of 300-keV electrons on semi-infinite CTA at several lateral distances from the beam center, for static irradiation.

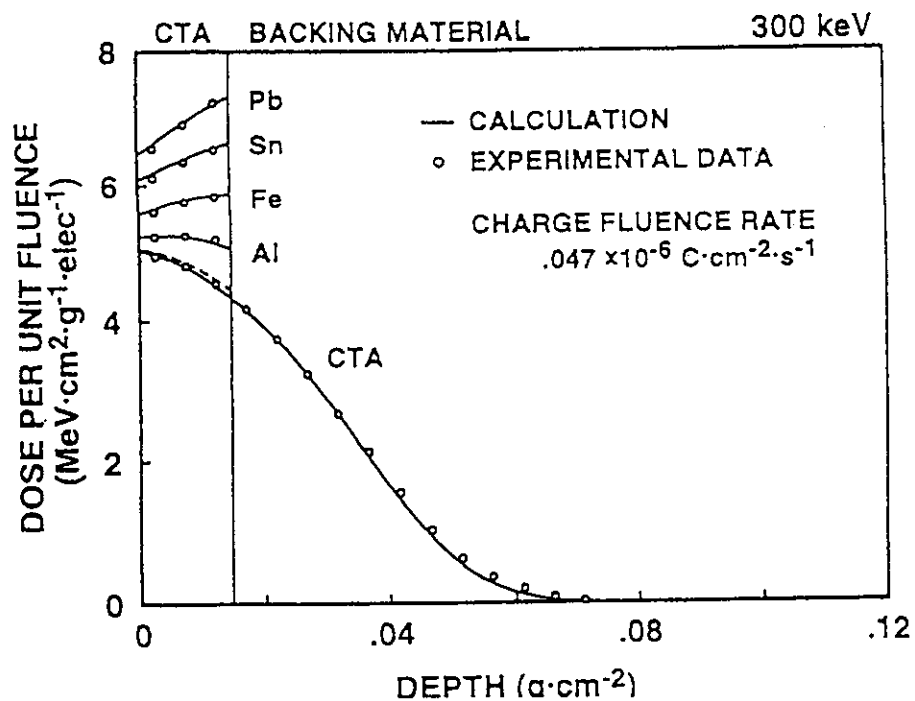


Fig. 5 Comparison of the calculated depth-dose distributions with the experiment for 300-keV electrons in a thin CTA stack on various backing materials.

15. Operation and Maintenance of Irradiation Facilities

K. Nakato

The irradiation facilities in our laboratory were operated for research performed in the laboratory and cooperative with universities and industries. Operation of the facilities was also made for irradiation service to industrial companies.

The Van de Graaff accelerator(No.1 accelerator) sometimes showed the accelerating voltage drop. But it was operated nearly satisfactory throughout the current year.

The accelerator of rectified transformer type(No.2 accelerator) and the cobalt-60 irradiation facility were operated satisfactory throughout the current year.

The annual operation of the facilities is given in Table 1.

Table 1 Utilization and operation of the facilities during fiscal 1993

	Van de Graaff accelerator (No. 1)	Accelerator of rectified transformer type (No. 2)	Cobalt 60 gamma ray source
Operation time	(hour:min) 181:47	(hour:min) 28:55	(hour:min) 4088:33
Number of experiments			
JAERI	95	52	184
Universities	0	0	0
Industries	29	0	13
Research Organizations	0	0	0
Total	124	52	197

III. List of Publications

1. Published Papers

M. Nishii, S. Sugimoto, Y. Shimizu, N. Suzuki, T. Nagase, M. Endo, and Y. Eguchi, "Surface Modification of Polytetrafluoroethylene Containing Carbonaceous Materials by KrF-Laser Irradiation", *Chem. Lett.*, 1993, 1063.

Y. Hamada, S. Kawanishi, M. Nishii, Y. Shimizu, S. Sugimoto, K. Ema, and T. Yamamoto, "Excimer Laser Irradiation Effects on Ethylene-Tetrafluoroethylene Copolymer", *J. Photopolym. Sci. Tech.*, 6, 385(1993).

S. Sugimoto, Y. Shimizu, and N. Suzuki, "Laser-Induced Reaction of CO-CH₄ Gaseous Mixture", *Chem. Express*, 8, 789(1993).

A. Okada, Y. Negishi, Y. Shimizu, S. Sugimoto, M. Nishii, and S. Kawanishi, "Endowment with the Wettability on the Surface of Tetrafluoroethylene-Perfluoroalkyl Vinyl Ether Copolymer by Excimer Laser Irradiation", *Chem. Lett.*, 1993, 1637.

Y. Shimizu, "Applications of Excimer Laser to Organic Chemical Reaction", *Radioisotopes*, 43, 147(1994).

T. Kijima and Y. Nakase, "Electron Beam Dosimetry for a Thin-layer Absorber Irradiated by 300-keV Electrons", *Appl. Radiat. Isot.*, 44, 693(1993).

K. Kaji, Y. Abe, M. Murai, N. Nishioka, and K. Kosai, "Radiation-Grafting of Acrylic Acid onto Ultrahigh Molecular High-Strength Polyethylene", *J. Appl. Sci.*, 47, 1427(1993).

M. Hatada, "Formation of Solid Particles from Aqueous Solutions of Palladium Sulfate and Palladium Sulfate-Silver Sulfate by Gamma Ray Irradiation", *JAERI-M* 93-232 (1993).

K. Kaji, I. Yoshizawa, C. Kohara, K. Komai, and M. Hatada, "Preparation of Flame-Retardant Polyethylene Form of Open-Cell Type by Radiation Grafting of Vinyl Phosphonate Oligomer", *J. Appl. Polym. Sci.*, 51, 84(1993).

L. Liu, T. Mitamura, M. Terasawa, and Y. Nakase, "Studies on the Radiation Damage of Metal Irradiated by Electron Beams", JAERI-memo 06-074 (1994).

2. Oral Presentations

Y. Hamada, S. Kawanishi, M. Nishii, Y. Shimizu, S. Sugimoto, K. Ema, and T. Yamamoto, "Excimer-Laser Irradiation Effects on Ethylene-Tetrafluoroethylene Copolymer", The 10th Photopolymer Conference (Tokyo), June 25, 1993.

Y. Shimizu, "Study of Organic Chemical Reaction Induced by Laser Radiation", Conference on Advanced Applications of Radiation (Osaka), July 5, 1993.

M. Nishii, "Surface Modification of Fluorine Resin by Laser Radiation", Conference on Advanced Applications of Radiation (Kyoto), August 24, 1993.

Y. Shimizu, S. Kawanishi, M. Nishii, S. Sugimoto, and N. Suzuki, "Photochemical Reaction of Organic Molecules-Hydrogen Peroxide by Intense Radiation from Excimer Laser", The 66th Annual Meeting (Autumn) of the Chemical Society of Japan (Nishinomiya), September 28, 1993.

A. Okada, Y. Negishi, Y. Shimizu, S. Sugimoto, M. Nishii, and S. Kawanishi, "Endowment with the Wettability on the Surface of Tetrafluoroethylene-Perfluoroalkyl Vinyl Ether Copolymer by Excimer Laser", The 66th Annual Meeting (Autumn) of the Chemical Society of Japan (Nishinomiya), September 28, 1993.

T. Nagase, M. Endo, M. Nishii, S. Sugimoto, Y. Shimizu, and S. Kawanishi, "Surface Modification of the Plasma-Treated PTFE Films by Excimer-Laser Irradiation", The 66th Annual Meeting (Autumn) of the Chemical Society of Japan (Nishinomiya), September 28, 1993.

T. Tanaka, Y. Eguchi, M. Nishii, S. Sugimoto, Y. Shimizu, and S. Kawanishi, "Modification of Wettability of PTFE Membrane with Excimer-Laser Irradiation", The 66th Annual Meeting (Autumn) of the Chemical Society of Japan (Nishinomiya), September 28, 1993.

- Y. Hamada, S. Kawanishi, M. Nishii, Y. Shimizu, S. Sugimoto, K. Ema, and T. Yamamoto, "Effects of Excimer-Laser Irradiation on Ethylene-Tetrafluoroethylene Copolymer", The 54th Annual Meeting of the Japan Society of Applied Physics (Sapporo), September 28, 1993.
- M. Endo and M. Nishii, "Improvement of Adhesive Properties of Fluoropolymers by Excimer Lasers", The 5th Radiation Processing Symposium (Osaka), November 25, 1993.
- M. Nishii, S. Sugimoto, Y. Shimizu, S. Kawanishi, N. Suzuki, T. Nagase, M. Endo, and Y. Eguchi, "Surface Modification of Polytetrafluoroethylene by KrF Laser", The 3rd Pacific Polymer Conference (Australia), December 14, 1993.
- M. Nagase, M. Endo, M. Nishii, S. Sugimoto, Y. Shimizu, and S. Kawanishi, "Irradiation Effects of Excimer Laser on Plasma-Treated Polytetrafluoroethylene", The 14th Symposium on The Laser Society of Japan (Chiba), January 21, 1994.
- Y. Shimizu, S. Kawanishi, and N. Suzuki, "Laser-Induced Photochemical Reaction of Aqueous Maleic Acid Solutions Containing H_2O_2 ", The 6th International Symposium on Advanced Nuclear Energy Research (Mito), March 24, 1994.
- S. Kawanishi, M. Nishii, Y. Shimizu, and S. Sugimoto, "Surface Modification of Polymer Materials by Excimer-Laser Irradiation", The 6th International Symposium on Advanced Nuclear Energy Research (Mito), March 24, 1994.
- S. Nakahashi, S. Arai, S. Sugimoto, and S. Kawanishi, "Calculation on Infra Red Multiphoton Decomposition Yield of Si_2F_6 ", The 67th Annual Meeting (Spring) of the Chemical Society of Japan (Tokyo), March 29, 1994.
- T. Nagase, M. Endo, M. Nishii, S. Sugimoto, and S. Kawanishi, "Improvement of Adhesive Properties by Excimer-Laser Irradiation of Fluorine Resin Applied with UV Absorbers", The 67th Annual Meeting (Spring) of the Chemical Society of Japan (Tokyo), March 31, 1994.
- A. Okada, Y. Negishi, Y. Shimizu, S. Sugimoto, M. Nishii, and S. Kawanishi, "Endowment with the Wettability on the Surface of Tetrafluoroethylene-Perfluoroalkyl Vinyl Ether Copolymer by Excimer Laser (2)", The 67th Annual Meeting (Spring) of the Chemical Society of Japan (Tokyo), March 31, 1994.

T. Kijima, Y. Nakase, and H. Suga, "Dose Distributions for 300-keV Electrons from a Scanning Type EB System", 1993 Autumn Meeting of the Institute of Electronics, Information and Communication Engineers, Sept. 27, 1993, Sapporo.

M. Hatada, "Formation of Solid Particles from Aqueous Solutions of Palladium Sulfate and Palladium Sulfate-Silver Sulfate by Gamma Ray Irradiation", The 36th Discussion Meeting of Radiation Chemistry, Oct. 8 1993(Hachioji).

I. Yoshizawa, C. Kohara, T. Shibata, G. Okumura, K. Kaji, and M. Hatada, "Modification of Polyethylene Form by Electron Beam Graft Copolymerization", The 5th Radiation Process Symposium, Nov. 24, 1993(Osaka).

T. Kijima, H. Suga, K. Nakato, and Y. Nakase, "Depth-Dose Distributions in a Thin Layer of Organic Absorber Irradiated by Low Energy Electrons", The 5th Radiation Process Symposium, Nov. 25, 1993(Osaka).

M. Hatada, "Formation of Solid Particles from Aqueous Solutions of Palladium Sulfate and Palladium Sulfate-Silver Sulfate by Gamma Ray Irradiation", The Discussion Meeting of Radiation-Induced Structure Changes, Dec. 13, 1993(Kumatori).

T. Kijima, H. Suga, and Y. Nakase, "Angular Distributions on a Sample Surface for 300-keV Electrons from EB System", 1994 Spring Meeting of the Institute of Electronics, Information and Communication Engineers, Mar. 26, 1994(Yokohama).

T. Kijima and Y. Nakase, "Dose-Estimation of Low Energy Electron Beam for Organic Thin Layer Absorbers", 1994 Annual Meeting (Spring) of the Atomic Energy Society of Japan, Mar. 29, 1994(Tsukuba).

3. Patent Applications

M. Nishii, Y. Shimizu, S. Kawanishi, S. Sugimoto, M. Endo, and T. Nagase, "A Method of Surface Modifying of Fluorine Resins", Japan Patent Appl., 5-258,087(1994).

S. Kawanishi, Y. Shimizu, M. Nishii, S. Sugimoto, and A. Okada, "Wettable Fluorine Resin", Japan Patent Appl., 5-265,964(1994).

M. Nishii, Y. Shimizu, S. Kawanishi, S. Sugimoto, T. Tanaka, and Y. Eguchi, "A Surface Modification of Polytetrafluoroethylene by KrF-Laser", US Patent Appl., 08/162, 702(1994).

IV. List of Cooperative Studies

Effect of laser beam irradiation on polymer materials

Faculty of Engineering, Osaka University

Infrared multiphoton decomposition of organofluorine compounds

Material Science and Technology, Kyoto Institute of Technology

Effects of laser irradiation on bio-related materials

Department of Preventive Dentistry, Ohu University

Surface modification of fluorine polymers by laser irradiation

Kurabo Industries, Ltd.

Improvement of vital affinity on fluorine polymers

Gunze Ltd.

Light emission from gases under electron irradiation

Osaka Electro-communication University

Distribution of trapped electrons in plastic thin layer(II)

Osaka Institute of Technology

Studies on the radiation-induced crosslinking of bio-degradable polymers

Institute of Bio-medical Engineering, Kyoto University

Lattice defects of silicon and germanium as studied by photo-luminescence and DLTS method

Naruto College of Education

Fine fabrication of functional membrane for separator(II)

Faculty of Engineering, Osaka University

Studies on the lattice-defects formation induced by electron irradiation

Faculty of Engineering, Himeji Institute of Technology

Formation of ultra-fine pattern in self-assembled multi-layers

Matsushita Electric Industries, Co.

Radiation-induced polymerization of composite thin layers

Daiwabou Kurieito Co. Ltd.

V. List of Personnel

Dr. Masafumi Nakano, director

Prof. Seizo Okamura, invited researcher

Dr. Motoyoshi Hatada, special principal scientist

OFFICE OF ADMINISTRATION

Mr. Teruo Yagi, administrative manager

Mr. Yasushi Tamura

Mrs. Atsuko Hayashi

Mrs. Harumi Ogata[8]

STUDY ON LASER-INDUCED ORGANIC CHEMICAL REACTIONS

Dr. Shunichi Kawanishi, leader

Mr. Yuichi Shimizu

Dr. Masanobu Nishii

Dr. Nobuyuki Ichinose

Mr. Shun'ichi Sugimoto[1]

Mr. Tomohiro Nagase[3]

Mr. Tadaharu Tanaka[3]

Mr. Atsushi Okada[3]

Mr. Yuji Hamada[4]

Mr. Shin-ichi Nakahashi[4]

STUDY ON BASIC RADIATION TECHNOLOGY FOR FUNCTIONAL MATERIALS

Dr. Yoshiaki Nakase, leader

Mr. Iwao Yoshizawa[2]

Dr. Norihisa Mino[3]

Dr. Kazufumi Ogawa[3]

Ms. Liu Li[4]

Mr. Hidetsugu Doi[6]

Mr. Keiichi Korekawa[6]

Mr. Masaaki Uehara[6]

Dr. C. D. Jonah[7]

OPERATION AND MAINTENANCE OF IRRADIATION FACILITIES

Mr. Kiyori Nakato, general manager

Mr. Toshiyuki Kijima[5]

- [1] Cooperative staff
- [2] Visiting researcher
- [3] Research collaborator
- [4] Student research assistant
- [5] Technical and research assistant
- [6] Thesis student
- [7] JAERI foreign researcher
- [8] Office assistant